Calcium isotopic variability of cervid bioapatite and implications for mammalian physiology and diet

A. Hassler, J. E. Martin, G. Merceron, M. Garel, V. Balter

This is an early version. Substantial changes in the content are available from the definitive version: https://doi.org/10.1016/j.palaeo.2021.110418

Calcium isotopic variability of cervid bioapatite and implications for mammalian physiology and diet

A. Hassler[1*] (auguste.hassler@ens-lyon.fr), J.E. Martin[1] (jeremy.martin@ens-lyon.fr), G. Merceron[2] (gildas.merceron@univ-poitiers.fr), M. Garel[3] (mathieu.garel@ofb.gouv.fr), V. Balter[1] (vincent.balter@ens-lyon.fr)

[1]Univ. Lyon, ENS de Lyon, Université Claude Bernard Lyon 1, CNRS, UMR 5276 Laboratoire de Géologie de Lyon : Terre, Planètes, Environnement, F-69007 46 Allée d'Italie, Lyon, France

[2]Laboratoire de Paléontologie, Évolution, Paléoécosystèmes, Paléoprimatologie (PALEVOPRIM; ex-iPHEP), UMR 7262 CNRS & Université de Poitiers, 86073 Poitiers Cedex 9, France

[3]Unité Ongulés Sauvages, Office Français de la Biodiversité (OFB; ex-ONCFS), 5 allée de Bethléem, Z.I. Mayencin, F-38610 Gières, France

*corresponding author

Abstract

There is clues that calcium (Ca) isotope composition of vertebrate bioapatite is influenced by diet and trophic level. These clues however conflict with several cases of mammal species exhibiting Ca isotope compositions which are inconsistent with their trophic levels. These observations support that diet may not be the only factor driving the Ca isotope composition in mammalian enamel and bone. To investigate this question, we selected a

modern *Cervus elaphus* population (Bauges Natural Regional Park, Alps, France) to serve as a model for Ca isotope physiology of cervids and other mammals. Subsequently, we reinvestigated the case of the fossil *Rangifer tarandus* population from Jaurens (Late Pleistocene locality, 32.6 to 29.7 kyr BP, France), a population for which abnormal ^{44}Ca-depleted isotope compositions have been previously documented. By combining bone samplings and serial enamel micro-samplings, we discuss the main potential sources of Ca isotopic variability in bioapatite of young and adult individuals. This includes the effects of gestation, lactation, antlerogenesis, browser-grazer ecologies, osteophagia and natural mineral licks. Our results highlight an important effect of lactation on bone Ca isotope composition ($\delta^{44/42}$Ca = +0.18 ± 0.07 ‰; 95 % confidence interval), whereas other factors such as gestation or antlerogenesis seem more secondary. Our enamel micro sampling method allowed to detect when enamel Ca isotope composition could be affected by milk consumption or mineral supplementation. Thanks to these advances, we collected new data from the Pleistocene reindeers of Jaurens which are now consistent with their apparent low trophic level (corresponding to a herbivorous diet). This demonstrates that disentangling ecological and physiological signals within enamel Ca isotope compositions is possible by using serial micro-sampling. This approach allows retrieving accurate trophic information from this proxy and which, altogether, truly push forward the limits of Ca isotope applications regarding paleoecology, physiology and ethology.

Keywords

Stable isotopes; Geochemistry; Paleoecology; Lactation, Mineral supplementation; Mammal physiology

1. Introduction

An increasing number of studies suggest that the stable Ca isotope composition of the hydroxylapatite of vertebrate bone and teeth, represents a record of diet within modern and fossil skeletal remains (Clementz et al., 2003; Chu et al., 2006; Reynard et al., 2010; Heuser et al., 2011; Clementz, 2012; Martin et al., 2015, 2017a, 2017b, 2018; Hassler et al., 2018). Body Ca originates mainly from food and water for land animals, but the Ca isotope composition of animals diverges from their food. At the opposite of carbon and nitrogen patterns, heavy Ca isotopes are discriminated against light Ca isotopes during their routing from food to tissues, notably in bone and enamel (Skulan and DePaolo, 1999; Chu et al., 2006; Hirata et al., 2008; Tacail et al., 2014; Heuser, 2016; Heuser et al., 2016). This results in a trophic level effect (hereafter TLE) with bones of herbivorous animals exhibiting more ^{44}Ca-depleted compositions compared to the plants they consume, and carnivorous predators following the same trend compared to their preys. This ultimately leads to an isotopic clustering of animal taxa in function of their trophic level, with primary consumers exhibiting a heavier Ca isotope composition than tertiary consumers, and secondary consumers exhibiting an intermediate isotopic composition. This has been observed in land ecosystems (Chu et al., 2006; Reynard et al., 2010; Martin et al., 2017a, 2018; Hassler et al., 2018; Dodat et al., 2021) and marine ecosystems (Clementz et al., 2003; Clementz, 2012; Martin et al., 2015, 2017b), even though for marine animals the Ca originating from seawater likely buffers dietary Ca intakes. These studies are based on ^{44}Ca/^{42}Ca or ^{44}Ca/^{40}Ca analyses of the hydroxylapatite of bone and teeth, commonly expressed as $\delta^{44/40}$Ca and $\delta^{44/40}$Ca, respectively (equivalent to the variation in ‰ compared to the Ca isotope ratios of a reference material, further detailed in section 2.6). Moreover, this technic allows to study the ecology of both modern and fossil specimens thanks to the good preservation potential of such mineralized

tissues and their Ca (Heuser et al., 2011; Martin et al., 2017a). This body of studies supports that Ca isotopes are a promising tool for diet and trophic inferences in modern and paleontological contexts with a large temporal range of action, providing the fact that mineralized tissues are preserved. However, inferring a TLE within mammalian communities relies on first order observations of Ca isotopic variability among predators and their preys. As highlighted in previous work, many uncertainties remain concerning the mechanisms behind fractionation processes as related to physiology versus environmental sources. As such, not all taxa are strictly following the theoretical isotopic/trophic clustering in the faunas studied so far. For some specific faunas and trophic niches, diet seems hard to constrain with Ca isotopes only (Reynard et al., 2010; Melin et al., 2014). Moreover, bone or enamel Ca isotope compositions sometime overlap between herbivores and predators, with herbivores occasionally exhibiting isotope compositions more ^{44}Ca-depleted than predators from the same fauna (e.g. hippopotamidae, mammoths and cervidae; see Martin et al., 2017a, 2018; Dodat et al., 2021). This raises important questions about what can generate such issues, and highlights how critical it is for the accurate use of this proxy to reconcile the evidences of TLE with the occasional decoupling recorded between trophic level and Ca isotope compositions.

The isotopic offset between diet and bone which generates the TLE ($\Delta^{44/42}Ca_{diet\text{-}bone}$) is relatively constant among mammal species with a value of -0.54 ± 0.08 ‰ (2 standard error, 20 individuals from 6 mammal species; reviewed in Tacail (2017)), despite resulting from the combination of numerous body Ca fluxes associated with Ca isotope fractionation (Skulan and DePaolo, 1999; Chu et al., 2006; Hirata et al., 2008; Tacail et al., 2014; Heuser et al., 2016; Tacail, 2017). The most impactful fluxes identified so far are the kidney Ca reabsorption from primary urines (Skulan et al., 2007; Heuser and Eisenhauer, 2010; Morgan

et al., 2012; Tacail et al., 2014; Channon et al., 2015; Heuser et al., 2016, 2019; Eisenhauer et al., 2019), the milk production and excretion (Chu et al., 2006; Reynard et al., 2010) and the bone mineralization (Skulan and DePaolo, 1999; Skulan et al., 2007; Heuser and Eisenhauer, 2010; Reynard et al., 2010; Morgan et al., 2012; Channon et al., 2015), although the significance of this last has been recently questioned (Tacail, 2017; Tacail et al., 2020). Changing these fluxes, like during gestation, lactation (Ramberg Jr et al., 1970; Cross et al., 1995; Giesemann et al., 1998; Karlsson et al., 2001; Wysolmerski, 2002; Vanhouten and Wysolmerski, 2003; Gallego et al., 2006; Kovacs and Fuleihan, 2006; Tacail, 2017) or antlerogenesis (Mitchell et al., 1976; Muir et al., 1987a, 1987b), likely modify the Ca isotopic equilibrium of the organism, the resulting $\Delta^{44/42}Ca_{diet\text{-}bone}$ offset, and could generate TLE discrepancies. Alternatively, the consumption of milk during nursing can also generate TLE discrepancies by changing the diet Ca isotope composition of non-weaned individuals compared to weaned individuals (Chu et al., 2006; Li et al., 2016, 2020; Tacail et al., 2017, 2019). Finally, Ca enriched mineral supplementation such as with mineral licks and osteophagia, as well as the Ca isotopic variability inherent to plants (Holmden and Bélanger, 2010; Gussone and Heuser, 2016; Schmitt, 2016; Moynier and Fujii, 2017; Martin et al., 2018; Griffith et al., 2020), are also able to blur the trophic clustering of Ca isotope compositions. The aim of this study is thus to investigate how these seven factors can affect bone and enamel Ca isotope compositions in modern animals, then to use this background to unravel a case study of TLE discrepancy previously documented.

We carried out the first part of this project by monitoring the bone and enamel Ca isotope compositions of a modern cervid population (red deer, *Cervus elaphus*), mainly originating from the Bauges Natural Regional Park (NRP), Alps, (Savoie, France). This modern population then served as a model to discuss TLE discrepancies, and more precisely

117 to discuss the case of the reindeers (*Rangifer tarandus*) from the Pleistocene locality of
118 Jaurens (Corrèze, France). Martin et al. (2017a) showed that reindeers from this locality
119 (dated between 32.6 to 29.7 kyr BP, Guérin et al. 1979) exhibit ^{44}Ca-depleted compositions in
120 tooth enamel down to a $\delta^{44/42}$Ca value of -1.75 ±0.09 ‰ (2 standard deviation.; 3 individuals).
121 This is different from the Ca isotope compositions of the other herbivores of this locality, and
122 closer from the one of lions and wolfs (Martin et al., 2017a). In accordance with the
123 documented effects of nursing on the body Ca isotope composition of the young (Chu et al.,
124 2006; Li et al., 2016, 2020; Tacail et al., 2017, 2019), Martin et al. (2017a) proposed that
125 these negative $\delta^{44/42}$Ca values could result from the consumption of maternal milk by reindeers
126 at the time when their analyzed molars were mineralizing (second molars, M2). Although this
127 hypothesis is tempting, no direct evidence was available to prove that this phenomenon was
128 responsible for the ^{44}Ca-depleted isotope composition reported among Jaurens fossil cervids,
129 leading to this new investigation.

130 To ensure the completion of our study it was necessary to assess at which degree the
131 Ca isotope composition of bone and enamel are comparable. Previous studies found
132 differences in $\delta^{44/42}$Ca values between bone and enamel or bone and enameloid (Heuser et al.,
133 2011; Tacail et al., 2014; Martin et al., 2015, 2017a), but it was unclear whether this offset
134 ($\Delta^{44/42}Ca_{bone\text{-}enamel}$) was due to different Ca isotope fractionation coefficient during
135 mineralization ($\alpha_{blood\text{-}bone}$ and $\alpha_{blood\text{-}enamel}$), to different mineralization timing, or to diagenesis.
136 Our modern red deer population is free of diagenetic influence, and therefore, mineralization
137 timings and differences between $\alpha_{blood\text{-}bone}$ and $\alpha_{blood\text{-}enamel}$ are the only factors affecting bone
138 and enamel Ca isotopic differences. In other words, characterizing $\alpha_{blood\text{-}bone}$ and $\alpha_{blood\text{-}enamel}$ in
139 red deer allow to accurately compare the different ontogenetic time periods recorded by these
140 two tissues.

2. Material and methods

2.1. Modern specimens

We studied a total of 21 specimens of wild red deer of two age classes (subadult and adult) and sex (10 males, 11 females), coming from Bauges NRP, Alps, (Savoie, France, 45.69 °N, 6.14 °E) and slaughtered during the hunting season in 2015 (between October and November) as part of the local hunting activity. In order to identify lactation, gestation and antlerogenesis effects on the Ca isotope composition of mineralized tissues, we analyzed and compared the bone Ca isotope composition of females and males. Our two age classes allow to distinguish specimens free of strong lactation, gestation and antlerogenesis effects (two years old, referred as subadult) from the others (aged of three years or more, referred as adult). Ages of the individuals were either known thanks to population monitoring or estimated based on tooth eruption and attrition stages (Brown and Chapman, 1991a, 1991b; table S1). The reproductive status of studied females was not directly monitored, but we know from observations of the OFB (Office Français de la Biodiversité) that in the red deer population of the Bauges NRP, 80 to 100 % of females aged of three years already gave birth at least once. Moreover, the OFB report that each year, about 80 % of the females aged of three years or more will have a fawn. We can refine this estimation as we know the body mass of studied specimens and that fertility is strongly related to body mass in cervids. Females are usually fertile when attaining 80 % of the adult body mass (Albon et al., 1986; Pellerin et al., 2014) and are around 30 % heavier at the end of autumn if they did not gave birth to a fawn earlier in the year (Mitchell et al., 1976; Clutton-Brock et al., 1982). These data allow to identify females which were too puny to be fertile, and females which were suspiciously too fat to have nursed a fawn recently. At the light of these data and knowing that the Bauges NRP deer population breed quite actively, we can confidently assume that adult females

weighting between 65 and 105 kg have given birth to a fawn during the 2015 birth season (table S1).

Bone samples were collected from mandibles, previously manually cleaned and boiled prior to be integrated to the collection of the PALEVOPRIM laboratory (UMR CNRS 7262 - University of Poitiers, France). For each mandible, bone sample powder was collected few centimeters under the second molar, with the help of a handheld drill (8200 Dremel equipped with a tungsten steel solid carbide bit). In order to remove any trace of dirt or other environmental contaminants, the first layer of bone surface was removed with the drill then cleaned with pure ethanol prior to sampling. Between 0.4 and 0.7 mg of bone powder were sampled and weighted prior to chemical preparation.

Along with bone sampling and in order to investigate intra-tissue and inter-tissue $\delta^{44/42}$Ca variability, we selected two specimens for serial enamel micro-sampling. The first is an adult male with premolars P2, P3, P4, and molars M1, M2, M3 fully emerged and moderately worn (specimen ID number: UP-15CE5672, lab name: AB). The second is a juvenile female with deciduous premolar DP2, DP3, DP4, and molars M1, M2 fully emerged and with an erupting M3 in ongoing mineralization (specimen ID number: UP-15CE3734, lab name: JVB). The serial micro-samplings performed on these specimens provide snapshots of the enamel Ca isotope composition at different ages, depending on when each enamel zone mineralized. This ultimately allows to identify isotopic anomalies produced by milk consumption, osteophagia, mineral licks or occasional consumption of ^{44}Ca-depleted plants. These deer specimens (AB and JVB), also had some plant leftovers trapped between their teeth. We collected these rests for elemental concentration analyses.

187 To assess the effect of antlerogenesis and antler consumption we selected an adult
188 male red deer preserved with its skull, mandible and antlers in the collections of the
189 Confluence Museum (Lyon, France). This specimen (ID number: MHNL-50002207, lab
190 name: SPB) is of unknown European origin and has been sampled following the same bone
191 sampling procedure than specimens from Bauges NRP. One sample has been retrieved from
192 the mandible, the other three were retrieved on the main beam of the right antler, respectively
193 at the base, the middle and the top of the antler.

194 *2.2. Fossil specimens*

195 In order to study the trophic position of reindeer from the Late Pleistocene Jaurens
196 fauna and their peculiar Ca isotope composition, we selected four specimens to carry out
197 serial enamel micro-sampling. We focused our efforts on enamel sampling instead of bones in
198 order to limit diagenesis influence. All specimens are part of the paleontological collections of
199 the Laboratory of Geology of Lyon (LGL-TPE, France). This includes two mandibles (one
200 adult and one juvenile) with their associated teeth, and two isolated teeth (lower M1 and a
201 lower DP4) from two different individuals. One of the two mandibles comes from an adult
202 specimen with the teeth P2, P3, P4, M1, M2, M3 fully emerged and with significant tooth
203 wear on the M1 (specimen ID number: FSL 451.409, lab name: AJ). The second mandible
204 comes from a juvenile specimen with the teeth DP2, DP3, DP4, M1 fully emerged and with
205 the M2 erupting (specimen ID number: FSL 451.389, lab name: JVJ). The isolated teeth are a
206 lower left DP4 (specimen ID number: FSL 451.398, lab name: ISO DP4) and lower right M1
207 (specimen ID number: FSL 451.384, lab name: ISO M1), both with a minimal wear level. The
208 lessons learned from modern specimens allow to critically discuss our new and previous
209 (Martin et al., 2017a) enamel Ca isotope data collected on fossil reindeers from Jaurens.

210 *2.3. Micro-sampling*

211 We designed two different procedures of serial micro-sampling. For both we use a
212 computer-assisted micro drill device (MicroMill), allowing the sampling of 80-120 µg
213 hydroxylapatite by drilling holes of 350–400 µm wide and about 400 µm depth. Teeth
214 selected for micro-sampling were serially sampled by micro-drilling on the enamel between
215 the apex (i.e. the top) and the neck of the tooth (i.e. the basal most enamel zone), along the
216 growth axis of the best preserved cusp of the lingual face. The apex is mineralizing first
217 whereas the enamel close to the neck is the last part of the enamel to mineralize. This
218 sampling thus maximizes the studied intra-tooth time window and allows a high temporal
219 resolution. When possible we performed serial micro-sampling using a "edge-drilling
220 procedure". In this case, the tooth (either isolated or extracted from a mandible) was cut along
221 the growth axis in the central part of the cusp by using a Buehler IsoMet Low Speed precision
222 sectioning saw with a diamond-studded circular saw blade. The edge of the enamel was then
223 polished using sandpaper with decreasing grain sizes prior to perform the micro sampling.
224 Sampling zones were located close to the enamel-dentine junction (EDJ) in order to minimize
225 the temporal lag between the mineralization of appositional structures and enamel maturation
226 (Blumenthal et al., 2014; Green et al., 2017; Trayler and Kohn, 2017; Müller et al., 2019).
227 Alternatively, when extracting and cutting teeth was impossible or when the targeted spatial
228 sampling resolution was sufficiently low, enamel has been micro-drilled from the outer side
229 ("outer-drilling procedure"). For this procedure, the one or two first hundreds of µm of drilled
230 enamel were not collected, in order to collect enamel relatively close to the EDJ similarly as
231 in the edge-drilling procedure. The choice of procedure is reported in table S1 and S2.

232 *2.4. Thin section and enamel age model*

233 We were allowed to make thin sections on the micro sampled surface of the M1 of
234 AB, JVB (red deer, Bauges) and ISO M1 (reindeer, Jaurens). Teeth were then sliced and
235 polished in order to obtain 100 µm thick sections. Observations in transmitted light
236 microscopy failed to reveal neonatal lines within the enamel layers of the three M1 (AB, JVB,
237 ISO M1), a structure observed in early mineralizing teeth of humans and other mammals that
238 would mark birth (Klevezal and Mina, 1995; Zanolli et al., 2011; Dean et al., 2019). The age
239 model necessary to anchor our enamel $\delta^{44/42}$Ca data was alternatively based on general
240 observations made on tooth mineralization timing of red deer (Brown and Chapman, 1991b).
241 Such data were not available for reindeer, but similarities between red deer and reindeer teeth
242 eruption timings (Miller, 1972; Brown and Chapman, 1991b; Azorit et al., 2002) allow to use
243 red deer data to build a coarse reindeer age model. As teeth are subject to wear, we spatially
244 anchored our age model on the neck of teeth. The mean mineralization age of each enamel
245 $\delta^{44/42}$Ca data point is then estimated based on the distance between the sampling zone and the
246 neck of the tooth, on corresponding mineralization timings (Brown and Chapman, 1991b),
247 and on the estimated full height of unworn teeth measured on young specimens. This method
248 assumes a constant enamel mineralization rate along the tooth growth axis and inside tooth
249 families. This method is thus not adapted to discuss inter-individual or intra-tooth differences
250 in tooth mineralization rates and timings but allow for a fairly good estimation considering
251 that enamel micro-samples average a body isotopic record spanning over a month to several
252 months (further discussed in appendix). For studied red deers, unworn teeth displayed similar
253 crown heights between specimens. Reindeer specimens, however, had unworn molars and
254 premolars approximately 15 % smaller than red deer, which has been considered in our age
255 model.

256 *2.5. Sample dissolution and ion chromatography*

257 Immediately after sampling, bone and tooth samples were transferred in Teflon
258 beakers. All further manipulations have been done exclusively in a clean lab or under a
259 laminar flux hood. Modern bone samples were dried with 500 µL of pure ethanol evaporated
260 at 70 °C. No attempt of leaching procedures has been carried out for fossil enamel samples, as
261 previous Ca isotope analyses demonstrated no isotopic differences between leached and non-
262 leached enamel in Jaurens samples (Martin et al., 2017a). All samples were dissolved using a
263 mix of 1 ml of 15 M ultrapure nitric acid (HNO_3) and 300 µL of ultrapure hydrogen peroxide
264 (30 %). Beakers were left closed at ambient temperature for 1h, then were heated at 130 °C
265 during 1 to 2 h more with regular degassing of nitrous fumes. When production of nitrous
266 fumes became limited, 300 µL of ultrapure hydrogen peroxide (30 %) were added and
267 samples were left to dry down at 90 °C for few hours. The presence of organic matter was
268 then tested using 100 µL of ultrapure hydrogen peroxide (30 %). No effervescence was
269 detected for any of the samples and solutions were thus left to dry down at 90 °C. Samples
270 selected for elemental concentration analyses were dissolved in 0.5 M ultrapure HNO_3 then
271 split. A fraction of the solution was reserved for concentration analyses and the rest was dried
272 down at 90 °C. These dried fractions and the samples not selected for concentration analyses
273 were kept for Ca isotope analyses, dissolved in 300-500 µL of 6M ultrapure hydrochloric acid
274 (HCl) and dried down at 90 °C.

275 The chromatography procedure used for Ca chemical purification is derived from
276 Tacail et al. (2014). This consist in a double column chromatography, starting with an elution
277 on AG 50WX-12 resin with ultrapure HCl, and followed by an elution on Eichrom Sr-specific
278 resin with an ultrapure HNO_3 medium. When high level of iron was suspected (e.g. fossil
279 samples) a third column chromatography was performed, using 1 mL of AG1 X8 resin and

following a procedure derived from Tacail et al. (2014). Blanks have been realized along the digestion and the chromatography, including total procedural blanks which have undergone all the steps previously described and chromatography blanks.

2.6. Analytical procedures and nomenclature

For more clarity within this paper, the n notation refers to the number of samples or specimens whereas the n* notation specifically refers to number of measurement replicates. The "s.d." notation refers to "standard deviation", whereas "s.e." refers to "standard error". Concentrations of major and trace elements were measured respectively on an inductively coupled plasma atomic emission spectrometer (ICP-AES) (ICAP 7400 Series, Thermo Scientific) and on an inductively coupled plasma mass spectrometer (ICP-MS) (ICAP-Q, Thermo Scientific). The reliability of measurements has been controlled through a set of blanks and reference material (SRM1486), and by replicating measures to n* = 2 for each sample.

We measured the Ca isotope ratios ($^{44}Ca/^{42}Ca$) using a multi-collector inductively coupled plasma mass spectrometer (MC-ICP-MS, Neptune Plus, Thermo Scientific) following the method described in Tacail et al. (2014). Prior Ca isotope analyses, Ca purified samples were dissolved and diluted in 0.05M HNO_3 in order to set the Ca concentration at 1.25 $mg.L^{-1}$. This concentration matches that of the ICP Ca Lyon, our in-house bracketing reference material made of Specpure Ca plasma standard solution (Alfa Aesar) and described in previous studies (Tacail et al., 2014, 2017; Martin et al., 2015, 2017a). Unless explicit mention, the Ca isotope compositions reported in this article are all expressed as $\delta^{44/42}Ca$ relatively to ICP Ca Lyon using the following formula:

$$\delta^{44/42}Ca = (((^{44}Ca/^{42}Ca)_{sample} / (^{44}Ca/^{42}Ca)_{ICP\ Ca\ Lyon}) - 1) \times 1000$$

304 For easing comparisons with studies using other reference materials, $\delta^{44/42}Ca_{\text{ICP Ca Lyon}}$ values
305 are converted to $\delta^{44/42}Ca_{\text{SRM915a}}$ in our tables and figures. Based on 71 measures synthetized in
306 the appendix of Martin et al. (2018), we converted $\delta^{44/42}Ca_{\text{ICP Ca Lyon}}$ values to $\delta^{44/42}Ca_{\text{SRM915a}}$
307 values by adding +0.518‰ to $\delta^{44/42}Ca_{\text{ICP Ca Lyon}}$ values. To express a difference of $\delta^{44/42}Ca$ value
308 between two Ca reservoirs we use the Δ notation based on the following formula:

309 $$\Delta x\text{-}y = \delta x - \delta y$$

310 Where x and y are different Ca reservoirs. Secondary reference materials of different matrix
311 and documented Ca isotope composition have been used to ensure the accuracy of our
312 analytical procedure and chemical purifications. The SRM1486 cow bone meal reference
313 material (NIST) was used in that purpose, as well as the IAPSO sea water (OSIL). The Ca
314 concentration of the blanks have also been measured with the Neptune Plus. Sample Ca
315 isotope compositions are considered different when their $\delta^{44/42}Ca$ mean value (±2 s.e.) do not
316 overlap. Groups of $\delta^{44/42}Ca$ mean values are compared using Wilcoxon rank-sum tests.

317 **3. Results**

318 *3.1. Trueness and precision*

319 Chromatography and total blanks display a maximum of 70 ng of Ca. This is several
320 thousand times less than the amount of Ca in our macro-samples (e.g. bone samples) which is
321 thus negligible. Most of our micro-samples (i.e. collected from spatial micro-sampling)
322 contained more than 6250 ng of Ca, and in the worst cases about 3800 ng of Ca. In this case
323 Ca from blanks is not completely negligible but its effect can be considered minimal. Indeed,
324 a simple mass balance calculation show that even a contamination with environmental Ca of
325 extreme isotopic composition (close to seawater ≈0.41 ‰; Martin et al. (2015)) affecting an
326 extremely ^{44}Ca-depleted sample (e.g. $\delta^{44/42}Ca$ = -2.00 ‰) with 3800 ng of Ca would only

generate a +0.04 ‰ difference. This unlikely +0.04 ‰ correspond to the maximum of contamination effect possibly expected with our blank levels for the smallest of our micro samples. Such effects can thus be neglected considering the order of magnitude of inter-sample differences discussed below.

The complete Ca isotope dataset of this study include 104 samples and reference materials for a total of 358 accurate measurements. The correlation between $\delta^{43/42}$Ca and $\delta^{44/42}$Ca values of each of these samples/reference materials follow the mass dependent relation expected for Ca isotope ratios (figure 1), with a slope value of 0.508 ± 0.010 (2 s.e) an intercept of 0.006 ± 0.015 (2 s.e) and a $R^2 = 0.99$ (p-value < 0.001). This demonstrates that no mass independent fractionation or mass specific interference has affected our measurements. Along with our different sessions of analysis, the SRM1486 exhibited a mean $\delta^{44/42}$Ca of -0.99 ± 0.13 ‰ (2 s.d. inter-session, n = 8 sessions) with a mean intra-session 2 s.d. of 0.08 ‰ (n = 88 measurements). Our other secondary reference material, the IAPSO exhibited a mean $\delta^{44/42}$Ca of +0.38 ± 0.12 ‰ (2 s.d. inter-session, n = 5 sessions) with a mean intra-session 2 s.d. of 0.06 ‰ (n = 14 measurements). These results are both in the range of previously published data (table S3) for the SRM1486 (Heuser and Eisenhauer, 2008; Tacail et al., 2016, 2017; Martin et al., 2018) and the IAPSO (Tacail et al., 2014; Martin et al., 2015). By considering all the measurements of samples and reference materials (n = 107), the mean intra-sample reproducibility was of ± 0.07 ‰ (2 s.d., n = 358 measurements).

3.2. Bone data among modern cervids

The bone sample set from Bauges NRP display a range of $\delta^{44/42}$Ca between -1.62 ± 0.19 ‰ (2 s.d., n* = 3) and -1.22 ± 0.04 ‰ (2 s.d., n* = 2), with a mean 2 s.d. of 0.09 ‰. Females red deer have a mean bone $\delta^{44/42}$Ca value of -1.36 ± 0.24 ‰ (2 s.d., n = 11), and males a mean bone $\delta^{44/42}$Ca value of -1.41 ± 0.27 ‰ (2 s.d., n = 10). The $\delta^{44/42}$Ca values of

351 female individuals are statistically indistinguishable from males when considering all age
352 classes together (Wilcoxon rank-sum test, p-value = 0.3494), but this change when
353 considering adult specimens only (Wilcoxon rank-sum test, p-value = 0.0499). Isolating
354 females who gave birth during the last birth season from the other females allows for an even
355 clearer distinction (figure 2). These six females (later referred as lactating hinds or females)
356 display bone $\delta^{44/42}$Ca values higher of +0.23 ± <0.01 ‰ (95 % confidence interval) compared
357 to the two adult females who did not reproduce recently (later referred as yeld hinds), and
358 differ significantly from adult males (Wilcoxon rank-sum test, p-value < 0.01; figure 3) with a
359 mean bone $\delta^{44/42}$Ca value higher of +0.17 ± 0.10 ‰ (95 % confidence interval). The three
360 subadult females display a range of bone $\delta^{44/42}$Ca values which overlap with both lactating and
361 yeld adult hinds, with the heaviest subadult females displaying the highest bone $\delta^{44/42}$Ca
362 values. Finally, the correlation between adult male body mass and bone $\delta^{44/42}$Ca values is
363 virtually absent (R = -0.29, p-value = 0.49, n = 8). We can make no distinction between bone
364 $\delta^{44/42}$Ca values of adult males and subadult males (Wilcoxon rank-sum test, p-value = 0.18) or
365 between adult males and subadult or yeld females (Wilcoxon rank-sum test, p-value = 0.62).

366 The SPB specimen displays a mandible bone $\delta^{44/42}$Ca value of -1.62 ± 0.04 ‰ (2 s.d.,
367 n* = 3), whereas the bone of the antler displays $\delta^{44/42}$Ca values of -1.43 ± 0.02 ‰ (2 s.d., n* =
368 4) at the base, -1.49 ± 0.06 ‰ (2 s.d., n* = 3) in the middle and -1.38 ± 0.06 ‰ (2 s.d., n* = 4)
369 at the top of the right antler (figure 4). Each of the antler $\delta^{44/42}$Ca values is significantly higher
370 from that of the mandible by 0.13 ‰ or more. Calcium and phosphorus concentrations
371 decrease from the base to the tip of the antlers, whereas magnesium reaches its maximum
372 concentration in the middle part of the antler (table S4).

373 *3.3. Enamel micro-samples*

374 Enamel and bone Ca isotope data of specimen AB (adult male) and JVB (juvenile
375 female) are reported in figure 5. Among these individuals, a majority of enamel $\delta^{44/42}$Ca values
376 of most adult parts of M3 and M2 teeth are undistinguishable from bone, whereas the DP4
377 (when present) and the early mineralizing part (next to the crown apex) of the M1 display
378 $\delta^{44/42}$Ca values which are -0.23 ‰ to -0.37 ‰ lower than bones. A similar difference is
379 observed within the M1 of the AB specimen, with early mineralizing parts exhibiting a
380 $\delta^{44/42}$Ca value -0.22 ‰ lower than late mineralizing parts. Plant remains found between tooth
381 cusps from AB and JVB display a Ca concentration of 1.83 wt% and 0.99 wt%, respectively.
382 The complete $\delta^{44/42}$Ca dataset of the specimens from the Bauges NRP is reported in table S1.

383 Enamel $\delta^{44/42}$Ca values of fossil reindeer (figure 6) range between -1.21 ± 0.04 ‰ (2
384 s.d., n* = 3) and -2.03 ± 0.08 ‰ (2 s.d., n* = 2). As for studied red deer, specimens with
385 unworn M1 (JVJ and ISO M1) exhibit an important change of $\delta^{44/42}$Ca values between early
386 and late mineralizing enamel. The earliest mineralizing part of the M1 display a $\delta^{44/42}$Ca value
387 lower by -0.82 ‰ for JVJ and by -0.47 ‰ for ISO M1 compared to last mineralizing part of
388 the M1. The enamel of the DP4 of JVJ display a $\delta^{44/42}$Ca value of -1.94 ± 0.06 ‰ (2 s.d., n =
389 3), undistinguishable from that of the earliest mineralizing part of its M1 (-2.03 ± 0.08 ‰, 2
390 s.d., n* = 2). Fluctuations of $\delta^{44/42}$Ca values during the adult life of reindeer are also observed
391 within the M3 and the P4 of the AJ specimen. The mean $\delta^{44/42}$Ca value measured on these two
392 teeth is -1.56 ± 0.19 ‰ (2 s.d., n = 3 for each tooth) with a total range of 0.22 ‰. The
393 complete $\delta^{44/42}$Ca dataset of the specimens from Jaurens is reported in table S2.

394 All three DP4 teeth display a pattern of low $\delta^{44/42}$Ca values, relatively stable from the
395 apex to the neck ($\Delta_{max\text{-}min}$ = 0.11 ‰; intra-teeth 2 s.d. = 0.11 ‰, n = 7). The M1 teeth display a
396 different pattern, with AB, JVJ and ISO M1 specimens exhibiting a high amplitude change

397 from low to high $\delta^{44/42}$Ca values from the apex to the neck ($\Delta_{max\text{-}min}$ = 0.50 ‰; intra-teeth 2 s.d.
398 = 0.35 ‰, n = 3). The M1 of JVB displays more stable low $\delta^{44/42}$Ca values ($\Delta_{max\text{-}min}$ = 0.17 ‰;
399 intra-teeth 2 s.d. = 0.12 ‰, n = 7), whereas the M1 of AJ displays stable $\delta^{44/42}$Ca values close
400 to its M2 and M3 $\delta^{44/42}$Ca values ($\Delta_{max\text{-}min}$ = 0.11 ‰; intra-teeth 2 s.d. = 0.12 ‰, n = 3).

401 **4. Discussion**

402 *4.1 Comparability of bone and enamel Ca isotope composition*

403 We observe some offsets of $\delta^{44/42}$Ca bone and enamel values in the M2 and M3 tooth
404 of AB and JVB specimens (figure 5), but theses offsets tend to be rarer after 5-6 months. The
405 fact that the late mineralizing enamel of the M2 and M3 of red deer specimens AB and JVB
406 display a $\delta^{44/42}$Ca value predominantly identical to their bones (figure 5), suggest that a similar
407 Ca isotope fractionation occur during bone and enamel mineralization (i.e. $\alpha_{blood\text{-}bone} \approx \alpha_{blood\text{-}}$
408 $_{enamel}$ and $\alpha_{diet\text{-}bone} \approx \alpha_{diet\text{-}enamel}$), despite that different cellular processes are involved. A similar
409 suggestion arises from human populations who exhibit M3 teeth with a $\Delta^{44/42}Ca_{diet\text{-}enamel}$ value
410 similar to the general mammal $\Delta^{44/42}Ca_{diet\text{-}bone}$ (Tacail et al., 2017), which suggest that this
411 could be a general feature among mammals or even vertebrates. These data consequently
412 support that $\Delta^{44/42}Ca_{bone\text{-}enamel}$ offset, when existing (Heuser et al., 2011; Tacail et al., 2014;
413 Martin et al., 2015, 2017a), are more likely caused by diagenetic alteration (for fossil tissues),
414 or by the different mineralization timings of enamel and bone. Indeed, in contexts of variable
415 body Ca isotope composition (e.g. forced by seasonal dietary variations), these different
416 mineralization timings generate different bone and enamel $\delta^{44/42}$Ca values, with bone sections
417 averaging years of body Ca isotope compositions and enamel micro-samples reflecting week
418 to month periods (see appendix section for further discussion of the length of these
419 mineralization periods).

4.2 Physiological control on $\delta^{44/42}Ca$ values in adult tissues

4.2.1 Gestation effects

In the red deer population from Bauges NRP, adult females who recently gave birth (referred as lactating hinds) display a mean bone $\delta^{44/42}Ca$ value of +0.17 ± 0.10 ‰ (95 % confidence interval) higher than adult males (figure 3). This is similar to what was previously reported for domestic sheep (Reynard et al., 2010), in which females (n = 8) displayed a bone $\delta^{44/42}Ca$ value significantly higher of +0.14 ± 0.08 ‰ (95 % confidence interval) compared to males (n = 16). The two factors pointed to be the cause of this sexual driven difference in sheep were the accretion of bone during gestation and the excretion of milk (Reynard et al., 2010), as only these two Ca fluxes were thought to be associated with Ca isotope fractionation at this time. However, the very low enamel $\delta^{44/42}Ca$ values we record in cervid teeth mineralizing *in utero* (DP4, early M1, figure 5 and 6) suggest that during gestation a mother will preferentially transfer light Ca isotopes through placental Ca transfer. This is also observed in human deciduous teeth (Tacail et al., 2017, 2019), although recent data point out that it could be representative of the last stage of gestation only (Li et al., 2020). Such trapping of isotopically light Ca by the foetus would have comparatively enriched mother tissues in heavy Ca isotopes (including mineralizing bone or enamel). The most simplistic box model of gestation (a 2 box model with a $\Delta^{44/42}Ca_{fawn\text{-}hind}$ of -0.25‰ and a hind giving 10% of her Ca to her fawn) gives a $\delta^{44/42}Ca$ shift of +0.02 to +0.03 ‰ for the hind, but it has to be noted that this model is very simplistic and amplifies the shift compared to reality (notably by neglecting Ca transfers from the foetus to the hind and the Ca intake of the hind). Among other changes, gestation also triggers higher Ca urinary excretions (Giesemann et al., 1998; Kovacs and Fuleihan, 2006; Reynard et al., 2010), a Ca flux which contributes to lower blood $\delta^{44/42}Ca$ values by preferentially exporting heavy Ca isotopes in urines (Skulan et al., 2007;

444 Heuser and Eisenhauer, 2010; Morgan et al., 2012; Tacail et al., 2014; Channon et al., 2015;
445 Heuser et al., 2016, 2019; Tacail, 2017; Eisenhauer et al., 2019). Thus, the consequences of
446 gestation have opposite influences on blood Ca isotope composition, and therefore limit the
447 record of a gestation signal in bone and enamel. Moreover, the recent questioning about the
448 $\alpha_{\text{blood-bone}}$ amplitude (Tacail, 2017; Tacail et al., 2020) also questions the base of the bone
449 accretion effect. Further investigations are necessary on this topic but at the moment these
450 sparse data tend to demonstrate that gestation has a weak to absent effect on body Ca isotope
451 compositions, and that bone differences between males and females recorded in red deer (this
452 study) and sheep (Reynard et al., 2010) have another origin. Similarly, nothing suggests that
453 gestation effects could significantly disrupt the trophic and isotopic clustering of adult bone
454 and enamel Ca isotope compositions.

455 *4.2.2 Lactation effects*

456 The amount of Ca provided by the hind to its fawn during the 3 to 8 months of nursing
457 is huge, as a fawn grows to about the half of the hind body mass between its birth and
458 weaning (table 1; table S1; Jones et al., 2009; Mitchell et al., 1976). Comparatively, a juvenile
459 red deer usually weights about 8 kg at birth (Mitchell et al., 1976; Jones et al., 2009) which
460 represents about 8.6 % of the mean body mass of adult hinds from our dataset (table S1) and
461 consequently implies far less Ca transfers from the hind to the fawn than lactation does. As
462 milk is very depleted in heavy Ca isotopes ($\Delta^{44/42}Ca_{\text{milk-diet}}$ = -0.6‰; Chu et al., 2006; Gussone
463 and Heuser, 2016; Heuser, 2016; Tacail, 2017), its excretion can lead to enrich lactating
464 females in Ca heavy isotopes (Reynard et al., 2010). Along with important Ca excretion
465 through milk, lactating mammals are subject to higher absorption in the digestive tract, to
466 bone loss and to changes in Ca urinary excretion (Ramberg Jr et al., 1970; Cross et al., 1995;
467 Giesemann et al., 1998; Karlsson et al., 2001; Wysolmerski, 2002; Vanhouten and

468 Wysolmerski, 2003; Kovacs and Fuleihan, 2006; Tacail, 2017). However, such Ca flux
469 changes likely secondarily affect the lactation signal, as these changes stay minimal compared
470 to the order of magnitude of milk excretion. The lactation should therefore be characterized
471 by higher body $\delta^{44/42}$Ca values in hinds, including within their bones if the nursing lasts for
472 several months (see appendix). In this context, the high bone $\delta^{44/42}$Ca values reported in
473 lactating hinds (figure 2 and 3) seems very compatible with the manifestation of a lactation
474 effect, similarly to what is observed for domestic sheep (Reynard et al., 2010). The important
475 residence time of Ca in bones certainly heavily damps this lactation signal (see appendix),
476 although the extensive bone remodeling and bone losses usually recorded during lactation
477 decreases this residence time and improves the potential of the signal to be recorded
478 (Giesemann et al., 1998; Vanhouten and Wysolmerski, 2003; Kovacs and Fuleihan, 2006).
479 Looking at subadult hinds for such a signal is more difficult, as their reproductive status is
480 challenging to assess and that only about 50 % gave birth to fawns at two years according to
481 OFB monitoring in Bauges NRP. However, higher body mass also suggests higher chance
482 that they gave birth to a fawn during the last birth season (Mitchell et al., 1976; Clutton-Brock
483 et al., 1982; Albon et al., 1986; Pellerin et al., 2014). Thus, the fact that bone $\delta^{44/42}$Ca values of
484 subadult females overlap with both lactating and yeld adult hinds suggest that this group
485 includes both nulliparous and primiparous females (figure 3). This is also consistent with the
486 fact that the heaviest subadult female displays the highest $\delta^{44/42}$Ca values, suggesting that this
487 specimen gave birth to a fawn during the last birth season.

488 Interestingly, the female with the highest body mass of our dataset displays lower bone
489 $\delta^{44/42}$Ca values despite having an age and body mass suggesting lactating periods in previous
490 birth seasons, as high body mass mean higher reproduction chances (Albon et al., 1986;
491 Pellerin et al., 2014). This suggests that skeletal Ca turnover is intense enough to conceal

42

492 lactation signals from one year to another in this species, at least within the cortical part of the
493 dentary bone (the bone part analyzed in this study). We lack precise data about bone
494 remodeling rate for red deer dentary bone. However, this fast Ca turnover seems odd
495 considering that the total skeleton would need about 9 years to remove 75 % of a lactation
496 signal (see box model described in appendix). The post-lactation bone accretion and the
497 relatively small male/female $\delta^{44/42}$Ca difference observed so far might help to achieve a
498 quicker concealing of the lactation signal, but further experiments are necessary to confirm
499 this dynamic as only one individual suggests this tendency. If bone Ca isotope composition
500 proves to be that dynamic, the time interval between last lactation and death, as well as the
501 time interval between consecutive lactations might be critical to preserve a lactation signal
502 within bone Ca isotope composition. Nevertheless, the amount of produced milk, the duration
503 of lactation periods and the size of the skeleton Ca reservoir also likely modulate this sex
504 driven Ca isotopic difference among mammal species. Those factors are probably a key to
505 explain why human populations studied by Reynard et al. (2010, 2013) display non-
506 significant isotopic clustering between sexes, along with the diversity of possible food sources
507 which characterize humans. Such lactation signal is in theory less dampened in enamel than in
508 bones (see appendix). However, looking for these signals in adult teeth of red deer females
509 seems challenging, as the enamel of the last tooth to mineralize (i.e. the M3) has generally
510 completed its mineralization around 26 months (Brown and Chapman, 1991b), while only
511 about half of two-year-old females are primiparous. We cannot be certain of that concerning
512 the reindeer population of Jaurens. However, our data suggest that any record of a lactation
513 signal within their enamel would result in higher enamel $\delta^{44/42}$Ca values, whereas these
514 reindeers exhibit suspiciously low $\delta^{44/42}$Ca values. We thus conclude that lactation effects on

44

515 body Ca isotope composition have to be considered when studying mammal populations but
516 cannot be invoked to explain anomalously low bone or enamel $\delta^{44/42}$Ca values.

517 *4.2.3 Antlerogenesis effects and antler records*

518 We report the first comparison between Ca isotope compositions of antlers and the rest
519 of the skeleton (figure 4). This pilot investigation highlights that antlers display $\delta^{44/42}$Ca values
520 significantly higher than the rest of the skeleton. As for enamel and bones, the key is to assess
521 whether this difference is the result from differences in Ca isotope fractionation coefficients at
522 mineralization or the result of a different mineralization timing. These data call for further
523 studies, as comparing antlers with bone and enamel could add an additional dimension for
524 studying cervid life history traits using Ca isotopes, allowing to further investigate diet
525 seasonality, for example.

526 With the only data presented in figure 4, it seems that antlers could preferentially trap
527 heavy Ca isotopes from blood, although physiological processes generally favor light Ca
528 isotopes (Tacail, 2017). If further confirmed, this would indicate that antlerogenesis could
529 lower body Ca isotope composition. Indeed, antlers act primarily as a Ca sink working
530 similarly as lactation and gestation by isolating Ca from the rest of the body, although antlers
531 are also subject to bone remodeling (Bélanger et al., 1967; Muir et al., 1987a; Rolf and
532 Enderle, 1999). However, the fact that lactation proved to have a relatively tenuous influence
533 on bone $\delta^{44/42}$Ca values, despite involving far bigger Ca fluxes and Ca isotope fractionation
534 coefficients than antlerogenesis (Mitchell et al., 1976; Muir et al., 1987a, 1987b; Harris et al.,
535 2002; Thomas and Barry, 2005; Li, 2013), suggests that antlerogenesis will not be detectable
536 within the skeleton Ca isotope composition. This is supported by the complete overlap we
537 observe between male red deer, yeld and immature hinds bone $\delta^{44/42}$Ca values (figure 3). An
538 overlap which occurs despite the fact that studied specimens have been slaughtered just when

539 the antlers of males finished their growth (Mitchell et al., 1976), so just when antlerogenesis
540 could had a strong influence on skeleton Ca isotope composition. Although further tests are
541 necessary to prove that enamel stay unaffected too, the end of enamel mineralization occurs
542 before large antlers can grow (Kruuk et al., 2002; Thomas and Barry, 2005) which suggests
543 that enamel will stay largely unaffected by antlerogenesis. In conclusion, none of our data
544 suggests that antlerogenesis could be an important driver of body Ca isotope compositions
545 and result in significant mismatch of Ca isotope compositions and trophic data.

546 *4.3 Nutrition control over bone and enamel $\delta^{44/42}$Ca values in modern and fossil cervids*

547 *4.3.1 Neonatal life history traits*

548 We discussed how gestation, lactation and antlerogenesis could affect adult bone and
549 enamel $\delta^{44/42}$Ca values, and neither of these phenomena can convincingly explain the low
550 $\delta^{44/42}$Ca values found in reindeer populations (Martin et al., 2017a). However, gestation and
551 lactation not only affect adult Ca isotope composition, they also control juvenile Ca intakes
552 and the Ca isotope composition of their tissues. For the 5 studied cervids with a preserved
553 DP4 or unworn M1 (AB, JVB, JVJ, ISO M1, ISO DP4), enamel mineralizing *in utero*
554 systematically exhibits the lowest $\delta^{44/42}$Ca values recorded (figure 5, 6). DP4 teeth exhibit
555 stable and low $\delta^{44/42}$Ca values relatively to third molars (M3) and adult bones, whereas M1
556 teeth exhibit various rates of transition from early ontogenetic low $\delta^{44/42}$Ca values to late
557 ontogenetic high $\delta^{44/42}$Ca values. A similar pattern of Ca isotope composition has been
558 previously described in human deciduous teeth, in which a clear link between weaning
559 practices and $\delta^{44/42}$Ca values has been described (Tacail et al., 2017). We thus propose that the
560 transition from low $\delta^{44/42}$Ca values in DP4 and in the apex of M1, to high $\delta^{44/42}$Ca values in the
561 neck of the M1, in the M2, M3 and adult bones is characteristic of the transition from
562 maternal Ca transfer (during the gestation then the nursing) to post-weaning Ca intake (adult-

like diet). The mineralization timing and enamel $\delta^{44/42}$Ca values of red deer and reindeer are consistent with the 3-8 months of weaning age of these species (Miller, 1972; Mitchell et al., 1976; Brown and Chapman, 1991b; Jones et al., 2009). The specimens AB, JVB and ISO M1 all reached adult Ca isotope composition at the neck of the M1. This suggests that they were weaned before four months considering the length of enamel mineralization (figure 5, 6 and appendix). Data from AJ (figure 6) also suggest a relatively early weaning, although the wear of the M1 limits the record of pre-weaning conditions. The JVB specimen constitutes an exception to this early transition of $\delta^{44/42}$Ca values in the M1. For this individual, the increase of $\delta^{44/42}$Ca values within the M1 seems flattened (see figure 5; $\Delta_{max\text{-}min}$ = 0.17 ‰; intra-tooth 2 s.d. = 0.12 ‰, n = 7), and enamel $\delta^{44/42}$Ca values only approach bone-like values within the M2 and M3 late mineralizing sections. This suggests a later weaning for this individual (around 8 months), or alternatively an earlier tooth mineralization. The fact that these weaning ages seem consistent with the observations of these species in the wild, supports that Ca isotopes are accurate for detecting *in utero*, milk feeding and weaning periods among mammals. These data also highlight that some individuals (like JVB) could display late dietary transition to purely adult diet (i.e. without milk), in a way that the transition is not yet complete when M2 teeth mineralize. This supports that milk consumption could have affected the previously published data of cervids from Jaurens (Martin et al., 2017a) and caused their suspiciously low enamel $\delta^{44/42}$Ca values. For these cervid species, we consequently advise to favor M3 enamel sampling to infer purely adult trophic information (when accessible). Note that in M3, enamel can then display higher $\delta^{44/42}$Ca values in case of an early breeding and subsequent lactation (see 4.2.2 section). When possible, we thus advise to analyze enamel zones which mineralized after weaning and prior to female sexual maturity. As the position of these zones are difficult to predict, especially for fossil species, we advise to use serial micro-

587 sampling in order to identify early post-weaning periods. This approach provides useful
588 complementary information for ecological and physiological inferences and minimizes the
589 potential of lactating females and nursing to affect trophic inferences based on $\delta^{44/42}$Ca data.

590 *4.3.2 Osteophagia and mineral licks*

591 Osteophagia (i.e. bone consumption) and the consumption of natural mineral licks are
592 two common sources of mineral supplementation that cervids, and more generally
593 artiodactyls, use during periods of high mineral requirement (e.g. lactation, juvenile growth,
594 antlerogenesis), notably to cope with phosphorus (P) or other element deficiency (Cowan and
595 Brink, 1949; Kjos-Hanssen, 1973; Krausman and Bissonette, 1977; Marie, 1982; Grasman
596 and Hellgren, 1993; Cáceres et al., 2011; Gambín et al., 2017). There is yet no direct measure
597 of mineral supplementation effects on enamel Ca isotope composition in the literature.
598 However, we can confidently assume that, because bones are generally ^{44}Ca-depleted
599 compared to plant products (Gussone and Heuser, 2016), antler or other bone consumption
600 will result in lower dietary $\delta^{44/42}$Ca values (Gussone and Heuser, 2016; Martin et al., 2017a,
601 2018). We can roughly estimate that this change of dietary $\delta^{44/42}$Ca value will be of 0 to -2‰,
602 depending of the amount of consumed bones and their Ca isotope compositions (Heuser et al.,
603 2011; Gussone and Heuser, 2016). Foraging on mineral licks would have the opposite effect
604 on dietary $\delta^{44/42}$Ca value (about 0 to +1 ‰), because soils and rocks are generally ^{44}Ca-
605 enriched compared to plant products (Gussone and Heuser, 2016). These modifications of the
606 dietary Ca isotope composition logically affect the $\delta^{44/42}$Ca values of growing enamel, with an
607 intensity that will depend upon the rate of enamel growth and the duration of the mineral
608 supplementation.

609 The resort to mineral supplementation by red deer from Bauges NRP has not been
610 quantified. However, we know from a red deer population from Spain that about two hundred

611 individuals can consume about 966 g of antlers over 7 months, mainly during lactation,
612 weaning and antlerogenesis periods (Estevez et al., 2008; Gambín et al., 2017). If we consider
613 that antlers contained a maximum of 15% of Ca (see appendix), this would represent about
614 0.7 g of Ca intake per individual. Considering that mineral supplementations were enhanced
615 by the low P availability in the plants of the study site in Spain (Estévez et al., 2009; Gambín
616 et al., 2017), we can expect a lower to similar intensity of mineral supplementations within
617 the Bauges NRP red deer population. Such Ca intakes seem negligible over a year compared
618 to plant and water sources, which suggests that mineral supplementations likely have a
619 negligible influence on bone $\delta^{44/42}$Ca values. However, few individuals may have been
620 responsible for most of this bone consumption (individuals were not identified in Gambín et
621 al. (2017)), and cervids from this study likely had access to other bones and mineral sources
622 than monitored antler stacks (Gambín et al., 2017). Therefore, it seems plausible to expect at
623 least short excursions in enamel $\delta^{44/42}$Ca values (negative for osteophagia, positive for mineral
624 licking) for individuals experiencing periods of important supplementation (i.e. lactation,
625 weaning, antlerogenesis). Following this postulate, we suspect that the outlier $\delta^{44/42}$Ca value
626 in the M3 of the JVB specimen has been influenced by osteophagia. This data point is
627 characterized by an isolated low $\delta^{44/42}$Ca value, localized far after weaning in enamel formed
628 around 15 months of age (figure 5), a period which could match the peak of supplementation
629 reported in September by Gambín et al. (2017). Finally, we note that the two latest M2
630 $\delta^{44/42}$Ca values of AB (at 10 months) seem slightly higher than the average M2, M3 and bone
631 $\delta^{44/42}$Ca values of this specimen (figure 5). It is possible that this results from Ca intakes
632 influenced by mineral licking, but the isotopic difference is tenuous, possibly artefactual, and
633 does not match with the common periods of mineral supplementation recorded in Spain
634 (Gambín et al., 2017).

635 Reindeer are also known to seasonally resort to mineral supplementation, likely to
636 compensate for the low P, Ca and sodium content of the plants and lichens they consume
637 (Grasman and Hellgren, 1993). Frequent antler chewing are reported in spring during the
638 calving season (Kjos-Hanssen, 1973; Marie, 1982), as well as mineral licks, notably in the
639 summer (Cowan and Brink, 1949). We have no data to quantify these supplementations, but it
640 seems reasonable to suspect they can influence enamel $\delta^{44/42}$Ca values. A possible example is
641 found within the M1 tooth of the JVJ specimen at 5 months (figure 6). This enamel zone
642 constitutes the terminal part of the weaning transition, and is characterized by a higher $\delta^{44/42}$Ca
643 value than within the M2 of the specimen (or of any other enamel sample from Jaurens
644 specimens). Because this critical period favors mineral supplementations in cervids (see
645 previous paragraph), we suspect that this positive $\delta^{44/42}$Ca excursion is the result of mineral
646 licking, although the very limited post-weaning JVJ dataset provides limited evidence for this.

647 If the effects of mineral supplementation on body Ca isotope composition are further
648 confirmed, this proxy could be used to study this crucial survival behavior among modern and
649 fossil mammals. As such, mineral supplementations however complicate the relation between
650 trophic level and enamel Ca isotope composition. Thus, we emphasize the importance of
651 considering mineral supplementation behaviors when using $\delta^{44/42}$Ca data for trophic
652 interpretations. We notably suggest a specific attention toward this behavior for the study of
653 artiodactyls from arid or tropical environments, because these environments are generally
654 marked by a low P availability in plants, a trigger for mineral supplementations (Grasman and
655 Hellgren, 1993).

656 *4.3.3 Plant Ca isotopic variability*

657 Identifying and excluding enamel $\delta^{44/42}$Ca data affected by pre-weaning, lactation and
658 short term mineral supplementation periods allow, with some limits (see previous section), to

identify Ca isotope data that are representative of trophic level. However, the important variability of plant Ca isotope compositions can also limit the trophic clustering of enamel and bone $\delta^{44/42}$Ca data, by generating isotopic variability among herbivores (Martin et al., 2018). Plant Ca isotope compositions combine a variability between plant organs and between plant taxa (Holmden and Bélanger, 2010; Gussone and Heuser, 2016; Schmitt, 2016; Moynier and Fujii, 2017; Martin et al., 2018; Griffith et al., 2020). The mean offset of -0.31 ± 0.14 ‰ observed between the leaves of dicotyledons and monocotyledons (e.g. grasses) is notably suspected to cause the documented difference of -0.18 ± 0.10 ‰ between the enamel of browser herbivores (i.e. with a leaf-dominated diet) and of grazer herbivores (i.e. with a grass-dominated diet) (Martin et al., 2018). Red deer is described as a mixed feeder, changing seasonally or regionally between more browser to more grazer diets (Hearney and Jennings, 1983; Gebert and Verheyden-Tixier, 2001; Storms et al., 2008; Berlioz et al., 2019). In the Bauges NRP, the grass proportion in the red deer diet has been estimated to change between 20 % and 40 % from summer to winter (Redjadj et al., 2014), and could be lower during late winter, spring and early summer according to the tendencies observed at the limits of monitored periods (Redjadj et al., 2014). Changing diet proportions from 40 % grass and 60 % leaves to 10 % grass and 90 % leaves would change the diet $\delta^{44/42}$Ca value of about 0.09 ‰, a result which is relatively close to the post-weaning range of 0.11 ‰ observed in the enamel record of the AB specimen (the red deer specimen with the most extensive post-weaning enamel record, figure 5). Our isotopic data are thus compatible, at the first order, with the known diet variability of this cervid population, although this estimation of 0.09 ‰ is built upon coarse approximations (notably that consumed grass $\delta^{44/42}$Ca value was exactly -0.31 ‰ lower than non-grass food $\delta^{44/42}$Ca value) and need further investigations. A higher resolution regarding the post-weaning enamel record, and a better constrain of the Ca isotope

683 composition of food items available at Bauges NRP (especially evergreen trees which are an
684 important food source for these red deer, Redjadj et al. (2014)) would provide $\delta^{44/42}$Ca data
685 that will be more comparable with δ^{13}C records, dental micro-wear and stomach content data
686 collected so far for this red deer population (Redjadj et al., 2014; Merceron et al., 2021). Such
687 further studies could notably help resolving some discrepancies between dental micro-wear
688 and stomach content estimations (i.e. higher versus lower grass content in the diet, Merceron
689 et al. (2021)), and provide independent complementary information regarding δ^{13}C data (e.g.
690 diet and ecological niche).

691 Reindeers are also mixed-feeders, but consume lichen during winter and have a
692 generally more browser diet compared to red deer (Hofmann, 1989; Mathiesen et al., 2000),
693 an observation which is notably consistent with the higher $\delta^{44/42}$Ca values of reindeers
694 compared to red deers when both co-exist within the same fauna (Dodat et al., 2021). After
695 weaning, the AJ specimen (the reindeer with the most extensive post-weaning enamel record)
696 exhibits a $\delta^{44/42}$Ca range of 0.25 ‰ (figure 6). As for red deer, this isotopic variability is
697 compatible, at the first order, with the consequences expected from changing proportions of
698 grass and other plant items in the diet. Within this browser to grazer-like diet continuum, the
699 lowest enamel $\delta^{44/42}$Ca values would correspond to more grazer-like diet periods, whereas
700 periods with the highest enamel $\delta^{44/42}$Ca values would correspond to more browser-like diet
701 periods. A limit to this hypothesis is the potential occurrence of mineral supplementations
702 which can modify the dietary Ca isotope composition independently of the plants (see section
703 4.3.3). In this regard, combining $\delta^{44/42}$Ca data and δ^{13}C data within a multi-proxy approach
704 (e.g. Martin et al., 2018) would be a solid option to further investigate diet and mineral
705 supplementation seasonality among these cervids.

706 *4.3.4 Trophic position of Pleistocene fossil cervids*

707 The previous discussion sections detail how to identify tooth and enamel parts that
708 should be favored for trophic inter-specific comparisons (by identifying pre- and post-
709 weaning periods, by detecting sections potentially disrupted by short term mineral
710 supplementation, and by providing insight about intra-tooth $\delta^{44/42}$Ca variability). We applied
711 this technic to three subadult to adult reindeers (AJ, JVJ, ISO M1) from the Late Pleistocene
712 locality of Jaurens. The most suited enamel data points for trophic inter-specific comparisons
713 are indicated in figure 6. Unfortunately, we do not have access to an extensive M2 and M3
714 dataset for JVJ and ISO M1 specimens (figure 6). Therefore, we lake insight to determine if
715 the enamel data points we selected for trophic inter-specific comparisons are entirely posterior
716 to the weaning transition. Nevertheless, the selected data points of these specimens
717 consistently range within the enamel Ca isotope compositions of AJ, which supports that they
718 are representative of a post-weaning diet. Altogether, the weighted average (per specimen) of
719 selected enamel $\delta^{44/42}$Ca values is +0.18 ‰ higher than previously published measures (Martin
720 et al., 2017a). They consequently plot within the range of woolly rhinoceroses (*Coelodonta*
721 *antiquitatis*, n = 3) (Wilcoxon rank-sum test, p-value = 0.1) and steppe bisons (*Bison priscus*,
722 n = 3; Wilcoxon rank-sum test, p-value = 0.2) published by Martin et al. (2017a). This
723 demonstrates that dismissing the data obtained from enamel affected by short term mineral
724 supplementation or milk consumption, based on a serial micro-sampling approach, efficiently
725 resolve the anomaly of ^{44}Ca depletion previously reported in the enamel of reindeers from
726 Jaurens. Serial micro-sampling is time and resource consuming and thus can hardly be used at
727 the scale of a whole faunal assemblage, but this study proves that this technique is particularly
728 suited to discuss of diet and behavior at the individual scale, or when some $\delta^{44/42}$Ca data are at
729 odds with independently inferred trophic positions or diet.

730 **5. Conclusions**

731 In this paper we discussed the behavioral and physiological events likely to affect
732 mammalian enamel and bone Ca isotope compositions, with two species of cervids as models
733 (*Cervus elaphus*, *Rangifer tarandus*). Our results highlight that lactation is an effective
734 source of Ca isotope variability as this phenomenon produced ^{44}Ca-enriched isotope
735 composition in bones of lactating females. Our study, however, failed to show any
736 comparable gestation effect, likely because of long Ca residence time in cervid bones, and
737 lower Ca fluxes or Ca isotope fractionation coefficients involved in cervid gestation.
738 Similarly, antlerogenesis did not prove to be a significant driver of body Ca isotope
739 composition in red deer. However, our data highlight that antlers display a different Ca
740 isotopic signature than the rest of the skeleton, encouraging further studies. The Ca
741 transferred from the cervid mother to the foetus during gestation has a similar isotope
742 composition than milk according to data from enamel mineralizing *in utero,* at least close
743 before birth. The transition from pre-parturition and pre-weaning Ca intakes to adult diet is
744 clearly observed within the enamel of most of the studied individuals. Calcium isotopes can
745 then be efficiently used for assessing weaning ages, providing the fact that no osteophagia is
746 involved early in life, as this phenomenon is also able to generate low bone and enamel
747 $\delta^{44/42}$Ca values (at the opposite of what is expected from mineral licks foraging). Finally, this
748 study demonstrates that serial micro-sampling of enamel is an appropriate method to
749 disentangle part of ecological, physiological and environmental Ca isotope signals. This
750 method allowed to accurately extract trophic information from the enamel $\delta^{44/42}$Ca values of
751 the reindeers from the Pleistocene deposit of Jaurens. When possible, we thus encourage the
752 use of this method in order to accurately retrieve diet and trophic signals from enamel $\delta^{44/42}$Ca
753 data. Such an approach would greatly benefit to paleoecology fields, as it makes Ca isotope

754 data more readily comparable with other diet proxy such as carbon and nitrogen isotopes.
755 Further studies are needed to investigate other cases of discrepancy between $\delta^{44/42}$Ca data and
756 trophic level, as well as to assess the variability of lactation, gestation and mineral
757 supplementation signals among mammals. However, these results open great perspectives for
758 the study of mammal physiology in addition to clarify the trophic inferences achievable with
759 Ca isotopes.

760 **Acknowledgements**

761 This research was supported by the TelluS program of CNRS/INSU (DIUNIS project
762 to JEM) and ENS de Lyon. We thank D. Mollex for his help regarding thin section
763 preparation, D. Berthet for allowing access to the specimen curated in the collections of the
764 Musée des Confluences , Lyon, and E. Robert for allowing access to Jaurens specimens
765 curated in the paleontological collections of the LGL-TPE. We would like to thank the
766 OGFH, the Groupement d'Intérêt Cynégétique des Bauges, the Office National des Forêts, as
767 well as the hunters and professionals from the ONCFS (T. Chevrier and T. Amblard) who
768 contributed to collect red deer data in Bauges NRP. Finally we thank the two reviewers, XXX
769 and XXX as well as the editor T. Tütken for their detailed comments that improved the initial
770 version of this work.

771 **References**

772 Albon, S.D., Mitchell, B., Huby, B.J., Brown, D., 1986. Fertility in female Red deer (*Cervus*
773 *elaphus*): the effects of body composition , age and reproductive status. J. Zool. 209,
774 447–460.

775 Azorit, C., Analla, M., Carrasco, R., Calvo, J.A., Muñoz-Cobo, J., 2002. Teeth eruption
776 pattern in red deer (*Cervus elaphus hispanicus*) in southern Spain. An. Biol. 24, 107–

777 114.

778 Bélanger, L.F., Choquette, L.P.E., Cousineau, J.G., 1967. Osteolysis in reindeer antlers;
779 Sexual and seasonal variations. Calcif. Tissue Res. 1, 37–43.
780 https://doi.org/10.1007/BF02008073

781 Berlioz, E., Azorit, C., Blondel, C., Ruiz, M.S.T., Merceron, G., 2019. Deer in an arid habitat:
782 dental microwear textures track feeding adaptability. Hystrix, Ital. J. Mammal. 28, 222–
783 230. https://doi.org/10.4404/hystrix

784 Biewener, A.A., 1990. Biomechanics of mammalian terrestrial locomotion. Science 250,
785 1097–1103. https://doi.org/10.1126/science.2251499

786 Blaine, J., Chonchol, M., Levi, M., 2015. Renal control of calcium, phosphate, and
787 magnesium homeostasis. Clin. J. Am. Soc. Nephrol. 10, 1257–1272.
788 https://doi.org/10.2215/CJN.09750913

789 Blumenthal, S.A., Cerling, T.E., Chritz, K.L., Bromage, T.G., Kozdon, R., Valley, J.W.,
790 2014. Stable isotope time-series in mammalian teeth : In situ $\delta^{18}O$ from the innermost
791 enamel layer. Geochim. Cosmochim. Acta 124, 223–236.
792 https://doi.org/10.1016/j.gca.2013.09.032

793 Brown, W.A.B., Chapman, N.G., 1991a. The dentition of red deer (*Cervus elaphus*): a scoring
794 scheme to assess age from wear of the permanent molariform teeth. J. Zool. London 224,
795 519–536.

796 Brown, W.A.B., Chapman, N.G., 1991b. Age assessment of red deer (*Cervus elaphus*): from
797 a scoring scheme based on radiographs of developing permanent molariform teeth. J.
798 Zool. London 225, 85–97. https://doi.org/10.1111/j.1469-7998.1991.tb03803.x

799 Cáceres, I., Esteban-Nadal, M., Bennàsar, M., Fernández-Jalvo, Y., 2011. Was it the deer or
800 the fox? J. Archaeol. Sci. 38, 2767–2774. https://doi.org/10.1016/j.jas.2011.06.020

801 Channon, M.B., Gordon, G.W., Morgan, J.L.L., Skulan, J.L., Smith, S.M., Anbar, A.D., 2015.
802 Using natural, stable calcium isotopes of human blood to detect and monitor changes in
803 bone mineral balance. Bone 77, 69–74. https://doi.org/10.1016/j.bone.2015.04.023

804 Chu, N.C., Henderson, G.M., Belshaw, N.S., Hedges, R.E.M., 2006. Establishing the
805 potential of Ca isotopes as proxy for consumption of dairy products. Appl. Geochem. 21,
806 1656–1667. https://doi.org/10.1016/j.apgeochem.2006.07.003

807 Clementz, M.T., 2012. New insight from old bones: stable isotope analysis of fossil
808 mammals. J. Mammal. 93, 368–380. https://doi.org/10.1644/11-MAMM-S-179.1

809 Clementz, M.T., Holden, P., Koch, P.L., 2003. Are calcium isotopes a reliable monitor of
810 trophic level in marine settings? Int. J. Osteoarchaeol. 13, 29–36.
811 https://doi.org/10.1002/oa.657

812 Clutton-Brock, T.H., Iason, G.R., Albon, S.D., Guiness, F.E., 1982. The effects of lactation
813 on feeding behavior in wild red deer hinds. J. Zool. London 198, 227–236.

814 Cowan, I.M., Brink, V.C., 1949. Natural game licks in the rocky mountain national parks of
815 Canada. Am. Soc. Mammal. 30, 379–387.

816 Cross, N.A., Hillman, L.S., Allen, S.H., Krause, G.F., Vieira, N.E., 1995. Calcium
817 homeostasis and bone metabolism during pregnancy, lactation, and postweaning: a
818 longitudinal study. Am. J. Clin. Nutr. 61, 514–523. https://doi.org/10.1093/ajcn/61.3.514

819 Dean, M.C., Spiers, K.M., Jan, G., Le Cabec, A., 2019. Synchrotron X-ray fluorescence
820 mapping of Ca, Sr and Zn at the neonatal line in human deciduous teeth reflects

821 changing perinatal physiology. Arch. Oral Biol.
822 https://doi.org/https://doi.org/10.1016/j.archoralbio.2019.05.024

823 Dodat, P.-J., Tacail, T., Albalat, E., Gomez-Olivencia, A., Couture-Veschambre, C., Holliday,
824 T., Madelaine, S., Martin, J.E., Rmoutilova, R., Maureille, B., Balter, V., 2021. Isotopic
825 calcium biogeochemistry of MIS 5 fossil vertebrate bones : application to the study of
826 the dietary reconstruction of Regourdou 1 Neandertal fossil. J. Hum. Evol. 151, 102925.
827 https://doi.org/10.1016/j.jhevol.2020.102925

828 Eisenhauer, A., Müller, M., Heuser, A., Kolevica, A., Glüer, C.C., Both, M., Laue, C., Hehn,
829 U. V., Kloth, S., Shroff, R., Schrezenmeir, J., 2019. Calcium isotope ratios in blood and
830 urine: A new biomarker for the diagnosis of osteoporosis. Bone Reports 10, 100200.
831 https://doi.org/10.1016/j.bonr.2019.100200

832 Estévez, J.A., Ceacero, F., Martínez, A., García, A.J., Landete-Castillejos, T., Gaspar-López,
833 E., López-Parra, J.E., Olguín-Hernández, C.A., Calatayud, A., Gallego, L., 2009.
834 Variación estacional en la composición mineral de plantas y su aplicación a la gestión
835 del ciervo ibérico, in: XXXIV Congreso Nacional de La Sociedad Española de
836 Ovinotecnia y Caprinotecnia (SEOC): Barbastro. Huesca, pp. 596–601.

837 Estevez, J.A., Landete-Castillejos, T., García, A.J., Ceacero, F., Gallego, L., 2008. Population
838 management and bone structural effects in composition and radio-opacity of Iberian red
839 deer (*Cervus elaphus hispanicus*) antlers. Eur. J. Wildl. Res. 54, 215–223.
840 https://doi.org/10.1007/s10344-007-0132-0

841 Ewbank, J.M., Phillipson, D.W., Whitehouse, R.D., Higgs, E.S., 1964. Sheep in the Iron Age:
842 a method of study. Proc. Prehist. Soc. 30, 423–426.
843 https://doi.org/10.1017/S0079497X0001519X

72

Fricke, H.C., Clyde, W.C., James, R.O., 1998. Intra-tooth variations in $\delta^{18}O$ (PO_4) of mammalian tooth enamel as a record of seasonal variations in continental climate variables. Geochim. Cosmochim. Acta 62, 1839–1850.

Gallego, L., Landete-Castillejos, T., Garcia, A., Sanchez, P.J., 2006. Seasonal and lactational changes in mineral composition of milk from Iberian red deer (Cervus elaphus hispanicus). J. Dairy Sci. 89, 589–595. https://doi.org/10.3168/jds.S0022-0302(06)72122-1

Gambín, P., Ceacero, F., Garcia, A.J., Landete-Castillejos, T., Gallego, L., 2017. Patterns of antler consumption reveal osteophagia as a natural mineral resource in key periods for red deer (Cervus elaphus). Eur. J. Wildl. Res. 63, 3–39. https://doi.org/10.1007/s10344-017-1095-4

Gebert, C., Verheyden-Tixier, H., 2001. Variations of diet composition of Red Deer (*Cervus elaphus* L.) in Europe. Mamm. Rev. 31, 189–201. https://doi.org/10.1046/j.1365-2907.2001.00090.x

Giesemann, M.A., Lewis, A.J., Miller, P.S., Akhter, M.P., 1998. Effects of the reproductive cycle and age on calcium and phosphorus metabolism and bone integrity of sows. J. Anim. Sci. 76, 796–807. https://doi.org/10.2527/1998.763796x

Grasman, B.T., Hellgren, E.C., 1993. Phosphorus nutrition in white−tailed deer: nutrient balance, physiological responses, and antler growth. Ecology 74, 2279–2296.

Green, D.R., Smith, T.M., Bidlack, F.B., Green, G.M., Colman, A.S., Tafforeau, P., 2017. Synchrotron imaging and Markov Chain Monte Carlo reveal tooth mineralization patterns. PLoS One 12, e0186391. https://doi.org/10.1371/journal.pone.0186391

866 Griffith, E.M., Schmitt, A.D., Andrews, M.G., Fantle, M.S., 2020. Elucidating modern
867 geochemical cycles at local, regional, and global scales using calcium isotopes. Chem.
868 Geol. 534, 119445. https://doi.org/10.1016/j.chemgeo.2019.119445

869 Guérin, C., Philippe, M., Vilain, R., 1979. Le gisement Pleistocène supérieur de la grotte de
870 Jaurens à Nespouls, Corrèze, France: historique et généralités. Nouv. Arch. du Muséum
871 D'Histoire Nat. Lyon 17, 11–16.

872 Gussone, N., Heuser, A., 2016. Biominerals and biomaterial, in: Hoefs, J. (Ed.), Calcium
873 Stable Isotope Geochemistry. Springer, Berlin, Heidelberg, pp. 111–144.

874 Hadjidakis, D.J., Androulakis, I.I., 2006. Bone remodeling. Ann. N. Y. Acad. Sci. 1092, 385–
875 396. https://doi.org/10.1196/annals.1365.035

876 Harris, R.B., Wall, W.A., Allendorf, F.W., 2002. Genetic consequences of hunting: What do
877 we know and what should we do? Wildl. Soc. Bull. 30, 634–643.

878 Hassler, A., Martin, J.E., Amiot, R., Tacail, T., Godet, F.A., Allain, R., Balter, V., 2018.
879 Calcium isotopes offer clues on resource partitioning among Cretaceous predatory
880 dinosaurs. Proc. R. Soc. B Biol. Sci. 285, 20180197.
881 https://doi.org/10.1098/rspb.2018.0197

882 Hearney, A.W., Jennings, T.J., 1983. Annual foods of the Red deer (*Cervus elaphus*) and the
883 Roe deer (*Capreolus capreolus*) in the east of England. J. Zool. 201, 565–570.

884 Heuser, A., 2016. Biomedical Application of Ca Stable Isotopes, in: Hoefs, J. (Ed.), Calcium
885 Stable Isotope Geochemistry. Springer, Berlin, Heidelberg, pp. 247–260.

886 Heuser, A., Eisenhauer, A., 2008. The calcium isotope composition ($\delta^{44/40}$Ca) of NIST SRM
887 915b and NIST SRM 1486. Geostand. Geoanalytical Res. 32, 311–315.

76

888 https://doi.org/10.1111/j.1751-908X.2008.00877.x

889 Heuser, A., Eisenhauer, A., 2010. A pilot study on the use of natural calcium isotope
890 ($^{44}Ca/^{40}Ca$) fractionation in urine as a proxy for the human body calcium balance. Bone
891 46, 889–896. https://doi.org/10.1016/j.bone.2009.11.037

892 Heuser, A., Eisenhauer, A., Scholz-Ahrens, K.E., Schrezenmeir, J., 2016. Biological
893 fractionation of stable Ca isotopes in Göttingen minipigs as a physiological model for Ca
894 homeostasis in humans. Isotopes Environ. Health Stud. 52, 633–648.
895 https://doi.org/10.1080/10256016.2016.1151017

896 Heuser, A., Frings-Meuthen, P., Rittweger, J., Galer, S.J.G., 2019. Calcium isotopes in human
897 urine as a diagnostic tool for bone loss: Additional evidence for time delays in bone
898 response to experimental bed rest. Front. Physiol. 10, 12.
899 https://doi.org/10.3389/fphys.2019.00012

900 Heuser, A., Tütken, T., Gussone, N., Galer, S.J.G., 2011. Calcium isotopes in fossil bones and
901 teeth - Diagenetic versus biogenic origin. Geochim. Cosmochim. Acta 75, 3419–3433.
902 https://doi.org/10.1016/j.gca.2011.03.032

903 Hirata, T., Tanoshima, M., Suga, A., Tanaka, Y., Nagata, Y., Shinohara, A., Chiba, M., 2008.
904 Isotopic analysis of calcium in blood plasma and bone from mouse samples by multiple
905 collector-ICP-mass spectrometry. Anal. Sci. 24, 1501–1507.
906 https://doi.org/10.2116/analsci.24.1501

907 Hofmann, R.R., 1989. Evolutionary steps of ecophysiological adaptation and diversification
908 of ruminants: a comparative view of their digestive system. Oecologia 78, 443–457.
909 https://doi.org/10.1007/BF02352565

910 Holmden, C., Bélanger, N., 2010. Ca isotope cycling in a forested ecosystem. Geochim.
911 Cosmochim. Acta 74, 995–1015. https://doi.org/10.1016/j.gca.2009.10.020

912 Jones, K.E., Bielby, J., Cardillo, M., Fritz, S.A., O'Dell, J., Orme, C.D.L., Safi, K., Sechrest,
913 W., Boakes, E.H., Carbone, C., Connolly, C., Cutts, M.J., Foster, J.K., Grenyer, R.,
914 Plaster, C.A., Price, S.A., Rigby, E.A., Rist, J., Teacher, A., Bininda-Emonds, O.R.P.,
915 Gittleman, J.L., Mace, G.M., Purvis, A., 2009. PanTHERIA: a species-level database of
916 life history, ecology, and geography of extant and recently extinct mammals. Ecology
917 90:2648.

918 Karlsson, C., Obrant, K.J., Karlsson, M., 2001. Pregnancy and lactation confer reversible
919 bone loss in humans. Osteoporos. Int. 12, 828–834.

920 Kjos-Hanssen, O., 1973. Reindeer antlers and what they can tell us about the reindeer
921 population. Nor. Archaeol. Rev. 6, 74–78.
922 https://doi.org/10.1080/00293652.1973.9965188

923 Klevezal, G.A., Mina, M. V., 1995. Recording structures of mammals : Determination of age
924 and reconstruction of life history. CRC Press.

925 Kohn, M.J., 2004. Comment: Tooth enamel mineralization in ungulates: Implications for
926 recovering a primary isotopic time-series, by B. H. Passey and T. E. Cerling (2002).
927 Geochim. Cosmochim. Acta 68, 403–405. https://doi.org/10.1016/S0016-
928 7037(03)00446-0

929 Kovacs, C.S., Fuleihan, G.E., 2006. Calcium and bone disorders during pregnancy and
930 lactation. Endocrinol. Metab. Clin. 35, 21–51. https://doi.org/10.1016/j.ecl.2005.09.004

931 Krausman, P.R.., Bissonette, J.A.., 1977. Bone-chewing behavior of desert mule deer.

932 Southwest. Nat. 22, 149–150.

933 Kruuk, L.E.B., Slate, J., Pemberton, J.M., Brotherstone, S., Guinness, F., Clutton-Brock, T.,
934 2002. Antler size in red deer: Heritability and selection but no evolution. Evolution (N.
935 Y). 56, 1683–1695. https://doi.org/10.1111/j.0014-3820.2002.tb01480.x

936 Li, C., 2013. Histogenetic aspects of deer antler development. Front. Biosci. 5, 479–489.

937 Li, Q., Nava, A., Reynard, L.M., Thirlwall, M., Bondioli, L., Müller, W., 2020. Spatially-
938 resolved Ca isotopic and trace element variations in human deciduous teeth record diet
939 and physiological change. Environ. Archaeol. 1–10.
940 https://doi.org/10.1080/14614103.2020.1758988

941 Li, Q., Thirlwall, M., Müller, W., 2016. Ca isotopic analysis of laser-cut microsamples of
942 (bio)apatite without chemical purification. Chem. Geol. 422, 1–12.
943 https://doi.org/10.1016/j.chemgeo.2015.12.007

944 Marie, W., 1982. Antlers-a mineral source in Rangifer. Acta Zool. 63, 7–10.

945 Martin, J.E., Tacail, T., Adnet, S., Girard, C., Balter, V., 2015. Calcium isotopes reveal the
946 trophic position of extant and fossil elasmobranchs. Chem. Geol. 415, 118–125.
947 https://doi.org/10.1016/j.chemgeo.2015.09.011

948 Martin, J.E., Tacail, T., Balter, V., 2017a. Non-traditional isotope perspectives in vertebrate
949 palaeobiology. Palaeontology 60, 485–502. https://doi.org/10.1111/pala.12300

950 Martin, J.E., Tacail, T., Cerling, T.E., Balter, V., 2018. Calcium isotopes in enamel of modern
951 and Plio-Pleistocene East African mammals. Earth Planet. Sci. Lett. 503, 227–235.
952 https://doi.org/10.1016/j.epsl.2018.09.026

953 Martin, J.E., Vincent, P., Tacail, T., Khaldoune, F., Jourani, E., Bardet, N., Balter, V., 2017b.

954 Calcium isotopic evidence for vulnerable marine ecosystem structure prior to the K/Pg
955 extinction. Curr. Biol. 1–4. https://doi.org/10.1016/j.cub.2017.04.043

956 Mathiesen, S.D., Haga, E., Kaino, T., Tyler, N.J.C., 2000. Diet composition, rumen
957 papillation and maintenance of carcass mass in female Norwegian reindeer (*Rangifer*
958 *tarandus tarandus*) in winter. J. Zool. 251, 129–138.
959 https://doi.org/10.1017/S0952836900005136

960 Melin, A.D., Crowley, B.E., Brown, S.T., Wheatley, P. V., Moritz, G.L., Yit Yu, F.T.,
961 Bernard, H., DePaolo, D.J., Jacobson, A.D., Dominy, N.J., 2014. Calcium and carbon
962 stable isotope ratios as paleodietary indicators. Am. J. Phys. Anthropol. 154, 633–643.
963 https://doi.org/10.1002/ajpa.22530

964 Merceron, G., Berlioz, E., Vonhof, H., Green, D., Garel, M., Tütken, T., 2021. Tooth tales
965 told by dental diet proxies: An alpine community of sympatric ruminants as a model to
966 decipher the ecology of fossil fauna. Palaeogeogr. Palaeoclimatol. Palaeoecol. 562,
967 110077. https://doi.org/10.1016/j.palaeo.2020.110077

968 Miller, F.L., 1972. Eruption and attrition of mandibular teeth in barren-ground caribou. J.
969 Wildl. Manage. 606–612.

970 Mitchell, B., McCowan, D., Nicholson, I.A., 1976. Annual cycles of body weight and
971 condition in Scottish Red deer, *Cervus elaphus* . J. Zool. 180, 107–127.
972 https://doi.org/10.1111/j.1469-7998.1976.tb04667.x

973 Morgan, J.L.L., Skulan, J.L., Gordon, G.W., Romaniello, S.J., Smith, S.M., Anbar, A.D.,
974 2012. Rapidly assessing changes in bone mineral balance using natural stable calcium
975 isotopes. Proc. Natl. Acad. Sci. U.S.A. 109, 9989–9994.
976 https://doi.org/10.1073/pnas.1119587109

84

Moynier, F., Fujii, T., 2017. Calcium isotope fractionation between aqueous compounds relevant to low-temperature geochemistry, biology and medicine. Sci. Rep. 7, 44255. https://doi.org/10.1038/srep44255

Muir, P.D., Sykes, A.R., Barrell, G.K., 1987a. Calcium metabolism in red deer (*Cervus elaphus*) offered herbages during antlerogenesis: Kinetic and stable balance studies. J. Agric. Sci. 109, 357–364. https://doi.org/10.1017/S0021859600080783

Muir, P.D., Sykes, A.R., Barrell, G.K., 1987b. Growth and mineralisation of antlers in red deer (*Cervus elaphus*). New Zeal. J. Agric. Res. 30, 305–315. https://doi.org/10.1080/00288233.1987.10421889

Müller, W., Nava, A., Evans, D., Rossi, P.F., Alt, K.W., Bondioli, L., 2019. Enamel mineralization and compositional time-resolution in human teeth evaluated via histologically-defined LA-ICPMS profiles. Geochim. Cosmochim. Acta 255, 105–126. https://doi.org/10.1016/j.gca.2019.03.005

Passey, B.H., Cerling, T.E., 2002. Tooth enamel mineralization in ungulates: Implications for recovering a primary isotopic time-series. Geochim. Cosmochim. Acta 66, 3225–3234. https://doi.org/10.1016/S0016-7037(02)00933-X

Pasteris, J.D., Wopenka, B., Valsami-Jones, E., 2008. Bone and tooth mineralization: Why apatite? Elements 4, 97–104. https://doi.org/10.2113/GSELEMENTS.4.2.97

Pellerin, M., Bonenfant, C., Garel, M., Chevrier, T., Queney, G., Klein, F., Michallet, J., 2014. Dynamique de la population de cerfs du domaine national de Chambord : Analyse temporelle des indicateurs de changement écologique (ICE). Rapp. d'expertise ONCFS.

Ramberg Jr, C.F., Mayer, G.P., Kronfeld, D.S., Phang, J.M., Berman, M., 1970. Calcium

999 kinetics in cows during late pregnancy, parturition, and early lactation. Am. J. Physiol.
1000 Content 219, 1166–1177.

1001 Redjadj, C., Darmon, G., Maillard, D., Chevrier, T., Bastianelli, D., Verheyden, H., Loison,
1002 A., Saïd, S., 2014. Intra- and interspecific differences in diet quality and composition in a
1003 large herbivore community. PLoS One 9. https://doi.org/10.1371/journal.pone.0084756

1004 Reynard, L.M., Henderson, G.M., Hedges, R.E.M., 2010. Calcium isotope ratios in animal
1005 and human bone. Geochim. Cosmochim. Acta 74, 3735–3750.
1006 https://doi.org/10.1016/j.gca.2010.04.002

1007 Rolf, H.J., Enderle, A., 1999. Hard fallow deer antler: A living bone till antler casting? Anat.
1008 Rec. 255, 69–77. https://doi.org/10.1002/(SICI)1097-0185(19990501)255:1<69::AID-
1009 AR8>3.0.CO;2-R

1010 Schmitt, A.-D., 2016. Earth-Surface Ca Isotopic Fractionations, in: Hoefs, J. (Ed.), Calcium
1011 Stable Isotope Geochemistry. Springer, Berlin, Heidelberg, pp. 145–172.

1012 Skulan, J., Bullen, T., Anbar, A.D., Puzas, J.E., Ford, L.S., LeBlanc, A., Smith, S.M., 2007.
1013 Natural calcium isotopic composition of urine as a marker of bone mineral balance. Clin.
1014 Chem. 53, 1155–1158. https://doi.org/10.1373/clinchem.2006.080143

1015 Skulan, J., DePaolo, D.J., 1999. Calcium isotope fractionation between soft and mineralized
1016 tissues as a monitor of calcium use in vertebrates. Proc. Natl. Acad. Sci. U.S.A. 96,
1017 13709–13713. https://doi.org/10.1073/pnas.96.24.13709

1018 Smith, C.E., 1998. Cellular and chemical events during enamel maturation. Crit. Rev. Oral
1019 Biol. Med. 9, 128–161.

1020 Smith, T.M., Austin, C., Green, D.R., Joannes-boyau, R., Bailey, S., Dumitriu, D., Fallon, S.,

1021 Grün, R., James, H.F., Moncel, M., Williams, I.S., Wood, R., Arora, M., 2018.
1022 Wintertime stress , nursing , and lead exposure in Neanderthal children. Sci. Adv. 4,
1023 eaau9483.

1024 Stevens, R.E., Balasse, M., O'Connell, T.C., 2011. Intra-tooth oxygen isotope variation in a
1025 known population of red deer: Implications for past climate and seasonality
1026 reconstructions. Palaeogeogr. Palaeoclimatol. Palaeoecol. 301, 64–74.
1027 https://doi.org/10.1016/j.palaeo.2010.12.021

1028 Storms, D., Aubry, P., Hamann, J.-L., Saïd, S., Fritz, H., Saint-Andrieux, C., Klein, F., 2008.
1029 Seasonal variation in diet composition and similarity of sympatric red deer *Cervus*
1030 *elaphus* and roe deer *Capreolus capreolus*. Wildlife Biol. 14, 237–250.
1031 https://doi.org/10.2981/0909-6396(2008)14[237:svidca]2.0.co;2

1032 Tacail, T., 2017. Calcium isotope physiology in mammals. PhD thesis. Université de Lyon.

1033 Tacail, T., Albalat, E., Télouk, P., Balter, V., 2014. A simplified protocol for measurement of
1034 Ca isotopes in biological samples. J. Anal. At. Spectrom. 29, 529.
1035 https://doi.org/10.1039/c3ja50337b

1036 Tacail, T., Le Houedec, S., Skulan, J.L., 2020. New frontiers in calcium stable isotope
1037 geochemistry: Perspectives in present and past vertebrate biology. Chem. Geol.
1038 https://doi.org/https://doi.org/10.1016/j.chemgeo.2020.119471

1039 Tacail, T., Martin, J.E., Arnaud-Godet, F., Thackeray, J.F., Cerling, T.E., Braga, J., Balter, V.,
1040 2019. Calcium isotopic patterns in enamel reflect different nursing behaviors among
1041 South African early hominins. Sci. Adv. 5, eaax3250.
1042 https://doi.org/10.1126/sciadv.aax3250

1043 Tacail, T., Télouk, P., Balter, V., 2016. Precise analysis of calcium stable isotope variations in
1044 biological apatites using laser ablation MC-ICPMS. J. Anal. At. Spectrom. 31, 152–162.
1045 https://doi.org/10.1039/C5JA00239G

1046 Tacail, T., Thivichon-Prince, B., Martin, J.E., Charles, C., Viriot, L., Balter, V., 2017.
1047 Assessing human weaning practices with calcium isotopes in tooth enamel. Proc. Natl.
1048 Acad. Sci. U.S.A. 114, 6268–6273. https://doi.org/10.1073/pnas.1704412114

1049 Thomas, D., Barry, S., 2005. Antler mass of barren-ground caribou relative to body condition
1050 and pregnancy rate. Arct. Inst. North Am. 58, 241–246.

1051 Trayler, R.B., Kohn, M.J., 2017. Tooth enamel maturation reequilibrates oxygen isotope
1052 compositions and supports simple sampling methods. Geochim. Cosmochim. Acta 198,
1053 32–47. https://doi.org/10.1016/j.gca.2016.10.023

1054 Vanhouten, J.N., Wysolmerski, J.J., 2003. Low estrogen and high parathyroid hormone-
1055 related peptide levels contribute to accelerated bone resorption and bone loss in lactating
1056 mice. Endocrinology 144, 5521–5529. https://doi.org/10.1210/en.2003-0892

1057 Wysolmerski, J.J., 2002. The evolutionary origins of maternal calcium and bone metabolism
1058 during lactation. J. Mammary Gland Biol. Neoplasia 7, 267–276.

1059 Zanolli, C., Bondioli, L., Manni, F., Rossi, P., Macchiarelli, R., 2011. Gestation length, mode
1060 of delivery, and neonatal line-thickness variation. Hum. Biol. 83, 695–713.
1061 https://doi.org/10.3378/027.083.0603

1062 **Table 1. Body mass data of red deer from Bauges NRP**

sex	age	mean	sd	n	lower	upper
F	A	98.05	12.82	447	81.58	114.52
F	J	52.00	8.75	223	40.73	63.27

92

F	SA	77.21	9.30	102	65.15	89.27
M	A	150.71	27.90	457	114.87	186.56
M	J	56.40	8.70	218	45.20	67.60
M	SA	96.05	13.66	187	78.44	113.66

1063

1064 NOTE. This table shows the total body mass data [kg] recorded on 1634 specimens of red
1065 deer from Bauges NRP. Age classes referred as adult (A), subadult (SA) and juvenile (J).

1066

1067 **Figures and captions**

1068 *Figure 1. Mass dependency*

1069 Three isotope plot: $\delta^{43/42}$Ca as a function of $\delta^{44/42}$Ca (‰, expressed relatively to ICP Ca Lyon)
1070 for all samples and standards analyzed for Ca isotope compositions in this study. The
1071 regression line of these Ca isotope compositions (central blue line) has a y-axis intercept of
1072 0.006 ± 0.015 (‰, 2 s.e.), indistinguishable from theoretical 0 ‰ intercept. The slope value of
1073 this line is 0.509 ± 0.016 (2 s.e.), indistinguishable from the 0.507 slope predicted by the
1074 exponential mass-dependent fractionation law (black dotted line). Error bars at the bottom
1075 right are average 2 s.d. for $\delta^{43/42}$Ca and $\delta^{44/42}$Ca. The two most external lines (blue) delimit the
1076 prediction interval whereas the two lines (red) around the central line correspond to the 95 %
1077 confidence interval of the regression line.

1078 *Figure 2. Sex and body mass control over bone $\delta^{44/42}$Ca values*

1079 Bone $\delta^{44/42}$Ca values of adult red deer specimens (≥ three years old) from Bauges NRP plotted
1080 in function of their total body mass. The average double standard error of these measures
1081 (Mean 2SE in the graph) is represented at the bottom right of the graph. The two vertical

94

1082 dotted lines mark the limits of body mass (65 and 105 kg) expected from females which
1083 supposedly gave birth and lactate during the last birth season preceding their death. Red deer
1084 silhouettes are modified from pictures of the public domain accessible in the following
1085 website: www.phylopic.org.

1086 *Figure 3. Sex and age control over bone $\delta^{44/42}$Ca values*

1087 Bone $\delta^{44/42}$Ca values of red deer from Bauges NRP grouped by sex and age categories. Adult
1088 red deer (≥ three years old) are represented by dots and sub-adults (two years old) by
1089 triangles. Boxplots are plotted from adult male and lactating female data. The degree of
1090 significance of the difference between these two groups is represented with stars (*), with two
1091 stars indicating a Wilcoxon rank-sum test: p-value < 0.01. The average double standard error
1092 of these measures (Mean 2SE in the graph) is represented at the bottom right of the graph.
1093 Red deer silhouettes are modified from pictures of the public domain accessible in the
1094 following website: www.phylopic.org.

1095 *Figure 4. Antler Ca isotopic composition*

1096 Intra-individual variability of mandible and antler bone $\delta^{44/42}$Ca values from the SPB
1097 specimen. In this graph antler micro-samples are plotted in function of their original position
1098 from the sampled antler displayed in photo. Blue error bars represent the 2 s.e. intervals of
1099 each sample. The horizontal black and red lines represent respectively the mean mandible
1100 bone $\delta^{44/42}$Ca value of the specimen and the limits of its confidence interval (± 2 s.e).

1101 *Figure 5. Enamel and bone $\delta^{44/42}$Ca variability of modern red deer*

1102 The $\delta^{44/42}$Ca values from bone and enamel micro-samples of AB and JVB specimens (modern
1103 red deer, Bauges NRP). The horizontal black and red lines represent respectively the mean
1104 bone $\delta^{44/42}$Ca value of each specimen and the limits of their confidence interval (± 2 s.e).

1105 Micro-samples from DP4, M1, M2 and M3 teeth are respectively represented by purple
1106 diamonds, red points, blue squares and green triangles. Dashed orange and cyan ellipses
1107 respectively emphasize periods during which mineral licking and osteophagia events are
1108 suspected. Error bares represent the 2 s.e. intervals for each sample. The age model used for
1109 temporally anchor enamel micro-samples is described in section 2.4 and is extrapolated from
1110 Brown and Chapman (1991a), with the only exception of enamel mineralizing *in utero* for
1111 which ages are arbitrary. Teeth mineralization timings which served this model are displayed
1112 at the bottom of the graph. Note that despite our micro-sampling procedure time averaging
1113 likely affects each of these enamel micro-samples (see appendix). Red deer silhouettes are
1114 modified from pictures of the public domain accessible in the following website:
1115 www.phylopic.org.

1116 *Figure 6. Enamel $\delta^{44/42}Ca$ variability of fossil reindeer*

1117 The $\delta^{44/42}Ca$ values from bone and enamel micro-samples of AJ, JVJ, ISO M1 and ISO DP4
1118 specimens (fossil reindeer). Note that ISO M1 and ISO DP4 are two distinct specimens that
1119 have been merged in one graph only for visual convenience. Micro-samples from DP4, M1,
1120 M2, M3 and P4 teeth are respectively represented by purple diamonds, red points, blue
1121 squares, green triangles and inverted yellow triangles. The dashed orange ellipse emphasizes a
1122 period during which mineral licking events are suspected. Dotted boxes contain points
1123 identified as providing accurate trophic information (see section 4.3). Error bares represent
1124 the 2 s.e. intervals of each sample. The age model used for temporally anchor enamel micro-
1125 samples is described in section 2.4 and is extrapolated from Brown and Chapman, 1991a,
1126 with the only exception of enamel mineralizing *in utero* for which ages are arbitrary. Teeth
1127 mineralization timings which served this model are displayed at the bottom of the graph. Note
1128 that despite our micro-sampling procedure time averaging likely affects each of these enamel

98

1129 micro-samples (see appendix). Reindeer silhouettes are pictures from the public domain
1130 accessible in the following website: www.phylopic.org.

1131 **Appendix**

1132 *Bone and enamel mineralization patterns*

1133 This appendix further describes the nature and length of mineralization we consider for bones
1134 and teeth. This text include the following references: (Ewbank et al., 1964; Biewener, 1990;
1135 Brown and Chapman, 1991a, 1991b; Smith, 1998; Fricke et al., 1998; Passey and Cerling,
1136 2002; Kohn, 2004; Hadjidakis and Androulakis, 2006; Pasteris et al., 2008; Stevens et al.,
1137 2011; Blaine et al., 2015; Tacail, 2017; Trayler and Kohn, 2017; Green et al., 2017; Smith et
1138 al., 2018).

1139 *Figure S1. Bone box model*

1140 This box model describes the evolution of a conceptual bone reservoir representing 1.2 x 10^6
1141 mg of Ca (in red) exchanging with an infinite reservoir (in purple) through 500 $mg.d^{-1}$ of input
1142 and output Ca fluxes. Bone starts with a $\delta^{44/42}Ca$ value of -0.5 ‰ and the infinite box is set to
1143 0 ‰. Time is given in days. These reservoir sizes are inspired from the human model
1144 described in Tacail (2017).

1145 *Table S1. Calcium isotope composition and supplementary information of red deer*

1146 This table includes all Ca isotope composition data collected on red deer in this study as well
1147 as additional specimen and sample details (e.g. sample ID, sampling method, body mass).
1148 When both data were available, total body mass was in average 1.28 bigger for males and
1149 1.42 bigger for females than their respective gutted body mass. We applied this factor to
1150 calculate the total body mass when only gutted body mass data were available. Total body
1151 mass format is in bold when weighted post mortem (i.e. not converted from gutted body

100

1152 mass). Age format is in bold when directly recorded, other age values are inferred from tooth
1153 eruption and attrition stages (Brown and Chapman, 1991a, 1991b).

1154 *Table S2. Calcium isotope composition and supplementary information of reindeer*

1155 This table includes all Ca isotope composition data collected on reindeer in this study as well
1156 as additional specimen and sample details (e.g. sample ID, sampling method).

1157 *Table S3. Calcium isotope composition of reference materials*

1158 This table includes all Ca isotope composition data collected in this study on SRM 1486
1159 (NIST) and IAPSO (OSIL). Data of the same reference materials from previous studies are
1160 summarized for comparison.

1161 *Table S4. Sample elemental composition*

1162 Sample elemental composition of 26 major and trace elements of herbaceous remains,
1163 mandibles and antlers.

102

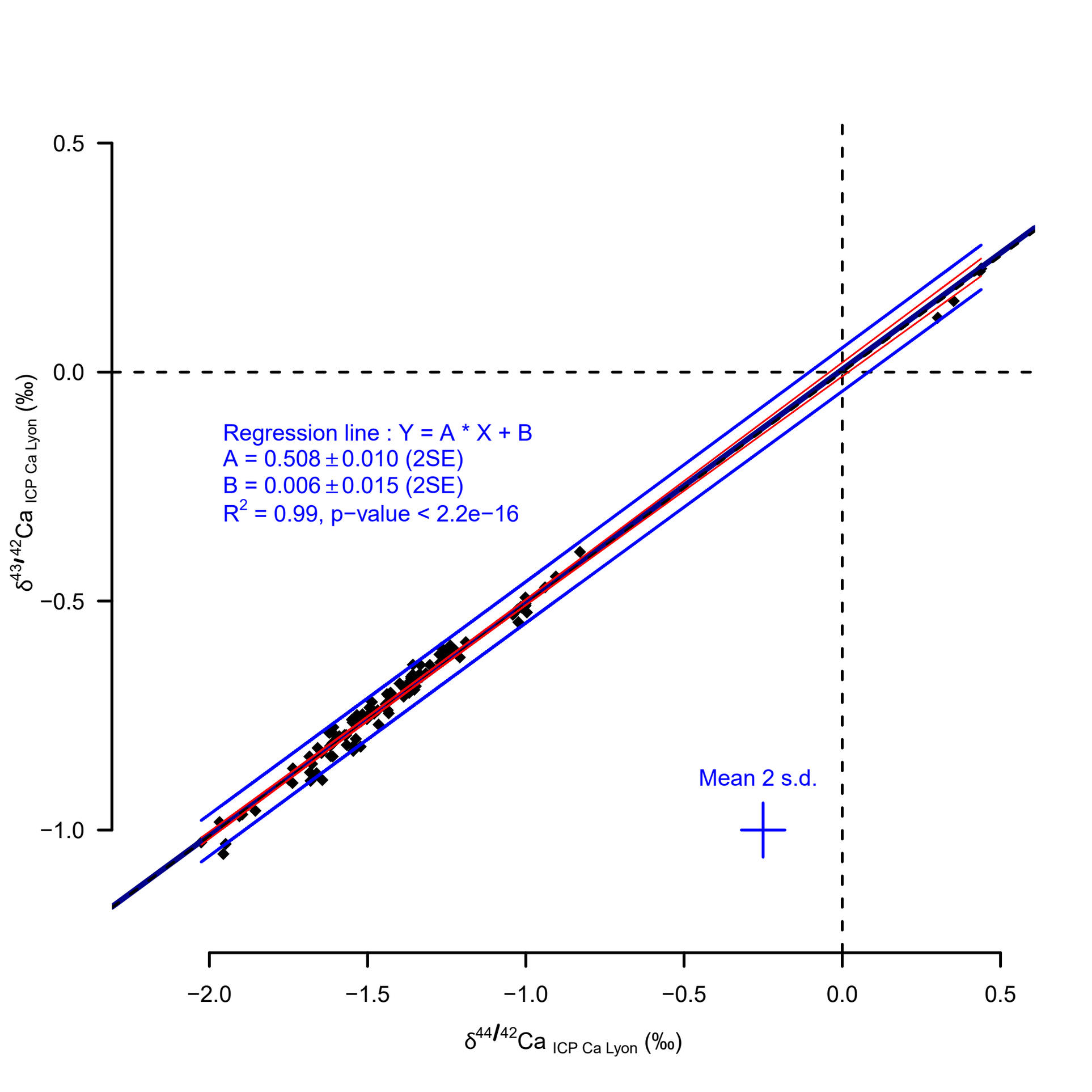
0.5
0.0
−0.5
−1.0
−2.0
−1.5
−1.0
−0.5
0.0
0.5
δ43/42Ca ICP Ca Lyon (‰)
δ44/42Ca ICP Ca Lyon (‰)
Regression line : Y = A * X + B
A = 0.508 ± 0.010 (2SE)
B = 0.006 ± 0.015 (2SE)
R2 = 0.99, p−value < 2.2e−16
Mean 2 s.d.

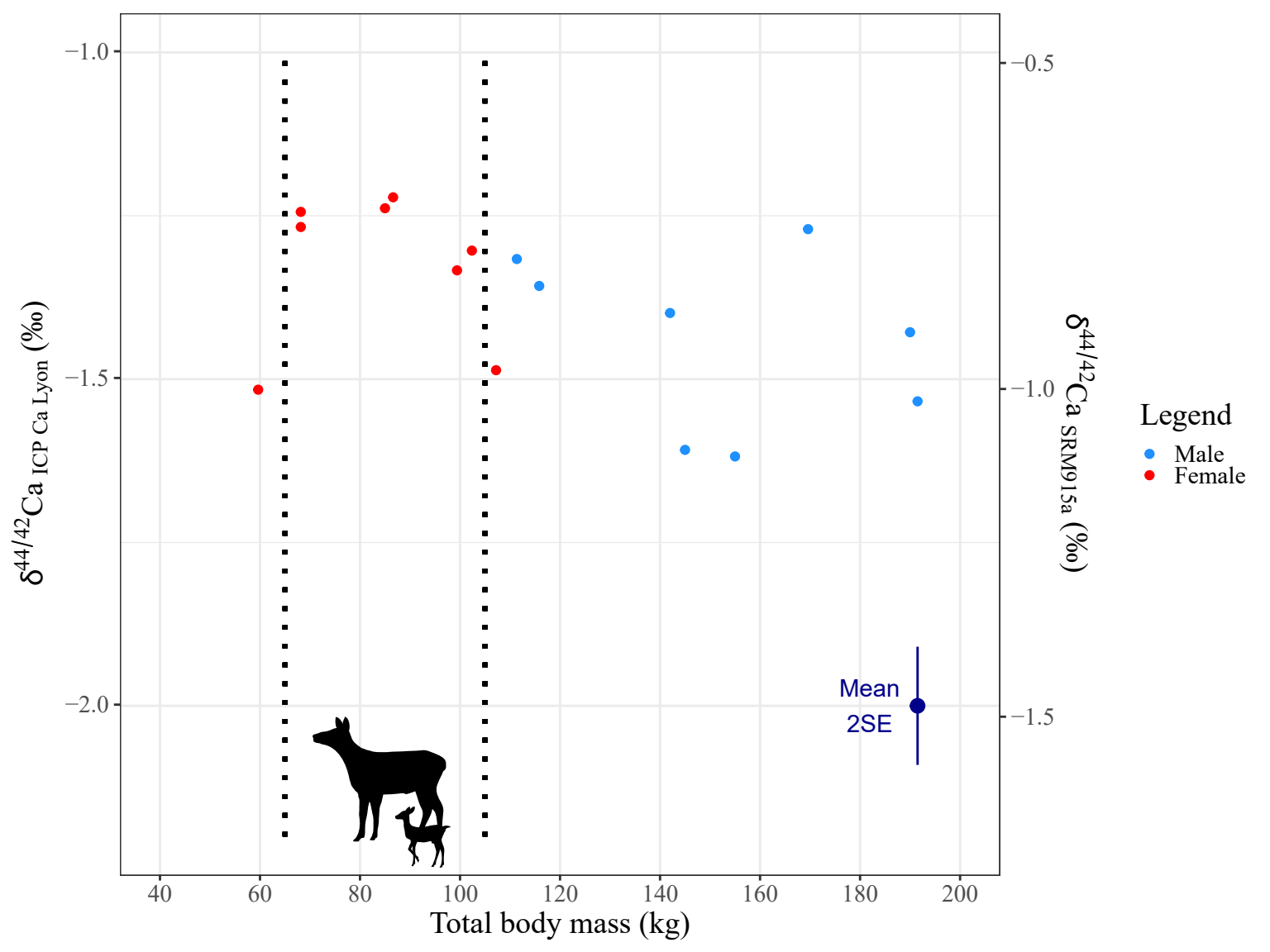
−1.0
−1.5
−2.0
−0.5
−1.0
−1.5
40
60
80
100
120
140
160
180
200
Total body mass (kg)
δ44/42Ca ICP Ca Lyon (‰)
δ44/42Ca SRM915a (‰)
Mean
2SE
Legend
Male
Female

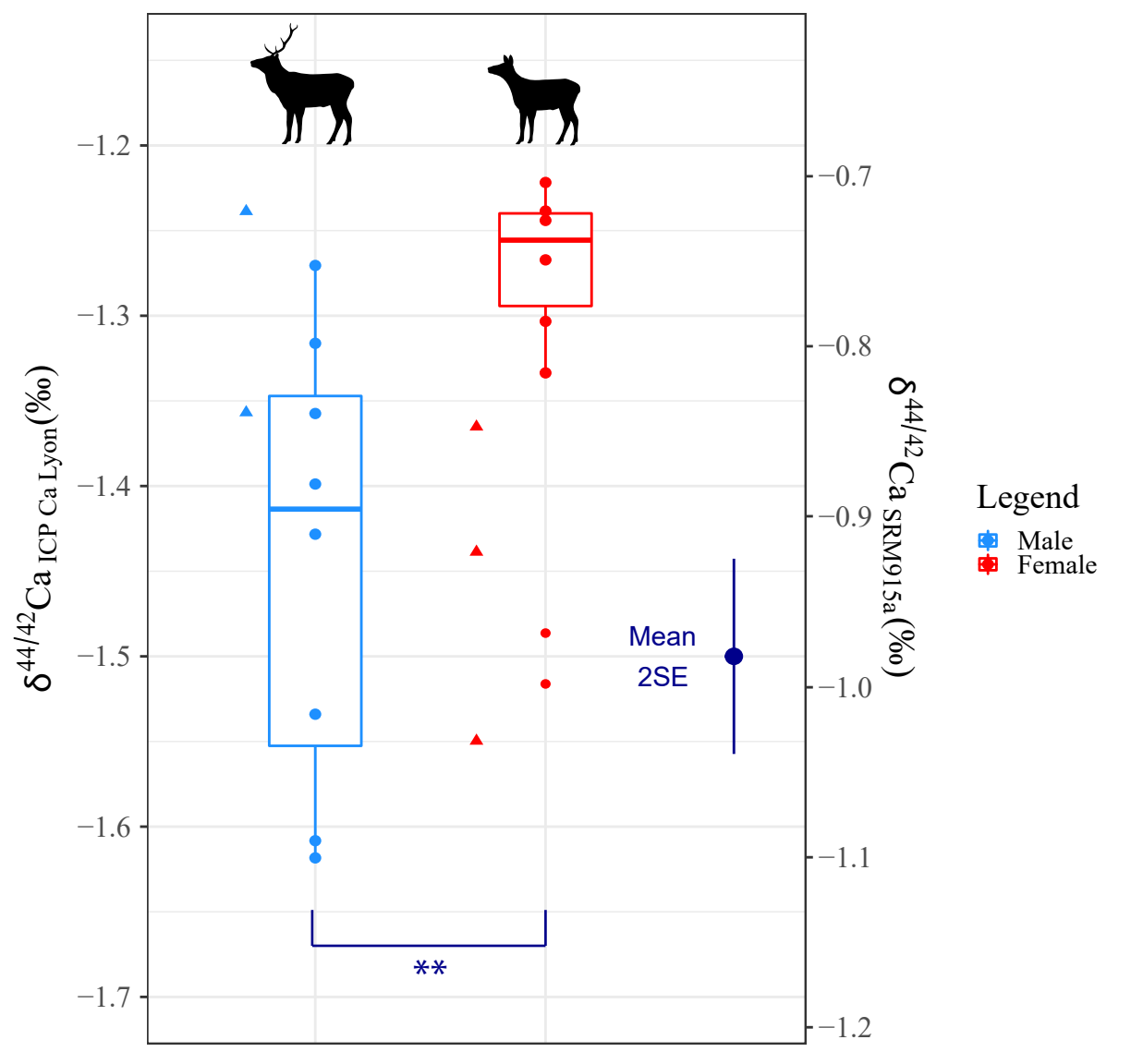
−1.2
−1.3
−1.4
−1.5
−1.6
−1.7
δ44/42Ca ICP Ca Lyon (‰)
−0.7
−0.8
−0.9
−1.0
−1.1
−1.2
δ44/42Ca SRM915a (‰)
Mean
2SE
**
Legend
Male
Female

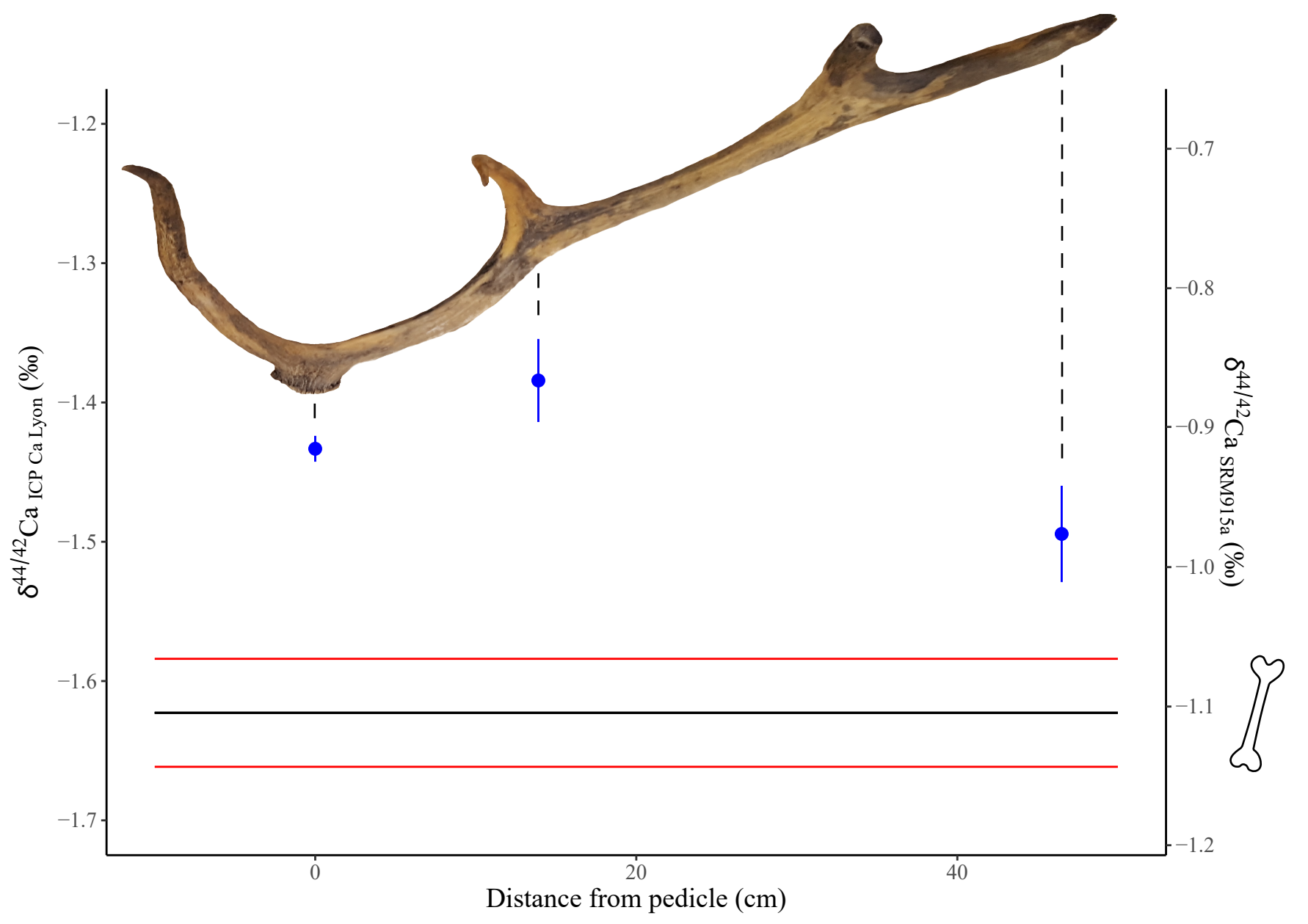
−1.2
−1.3
−1.4
−1.5
−1.6
−1.7
δ44/42Ca ICP Ca Lyon (‰)
−0.7
−0.8
−0.9
−1.0
−1.1
−1.2
δ44/42Ca SRM915a (‰)
0
20
40
Distance from pedicle (cm)

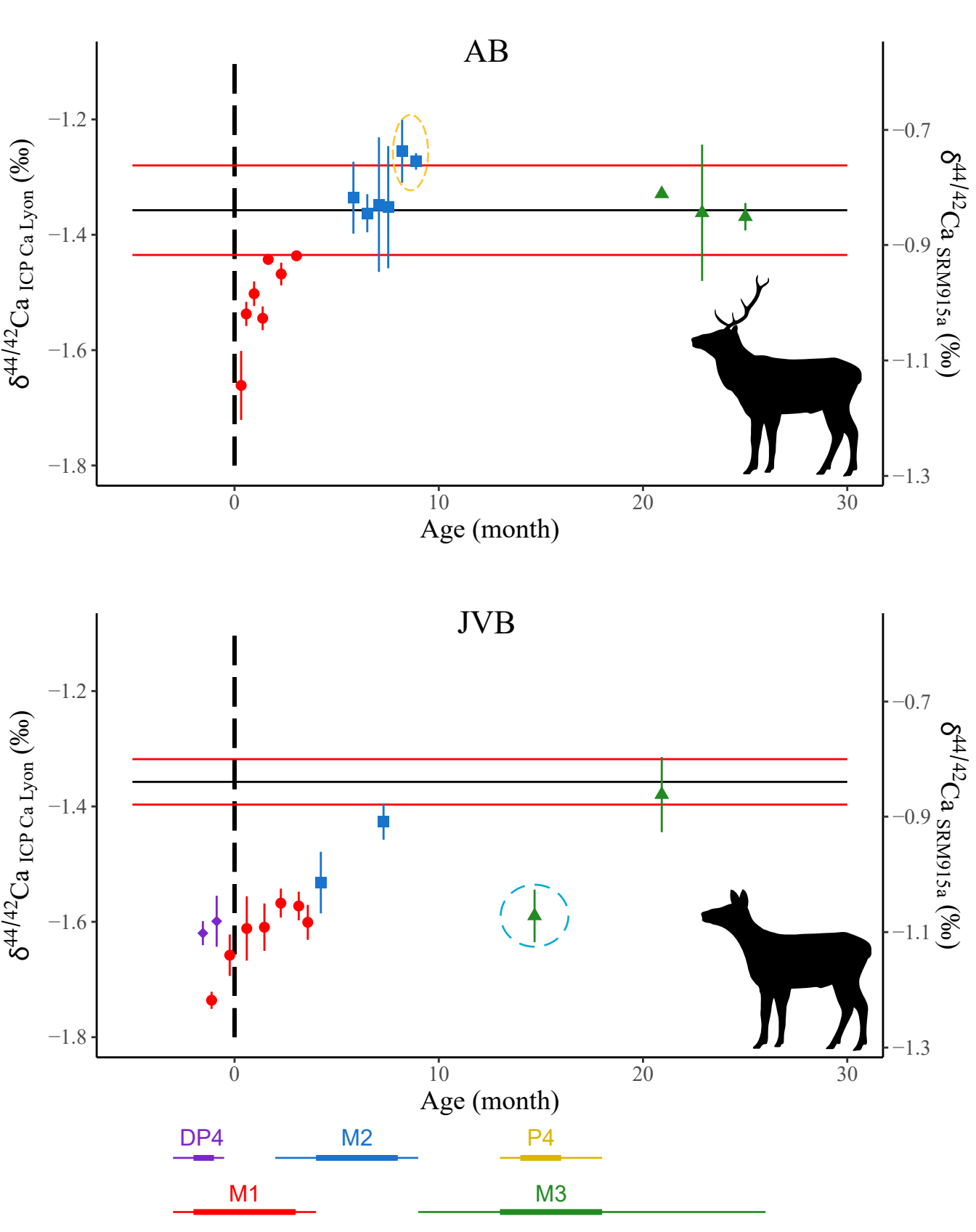
AB
JVB
δ44/42Ca ICP Ca Lyon (‰)
δ44/42Ca SRM915a (‰)
−1.2
−1.4
−1.6
−1.8
−0.7
−0.9
−1.1
−1.3
0
10
20
30
Age (month)
DP4
M2
P4
M1
M3

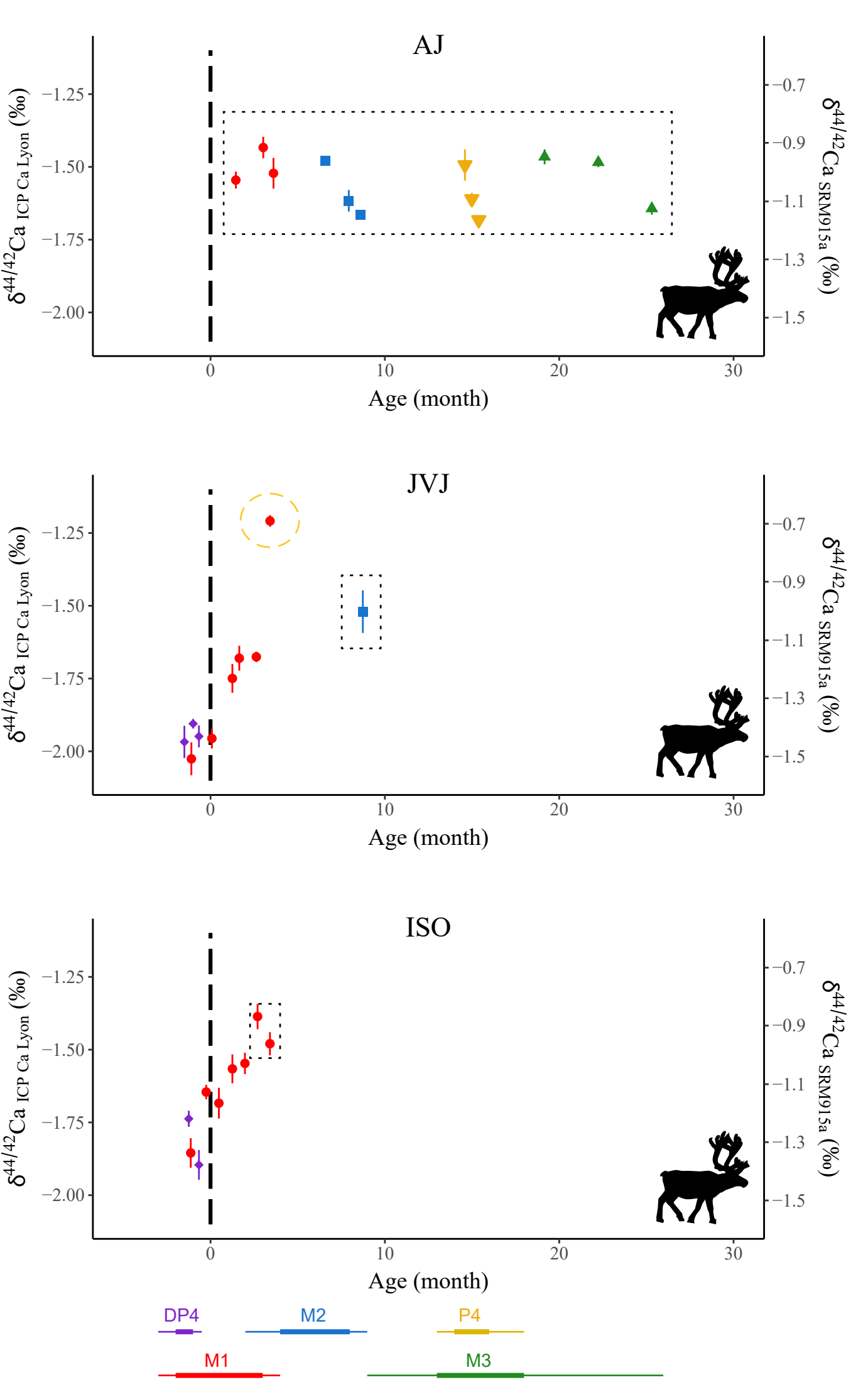
AJ
JVJ
ISO
δ44/42Ca ICP Ca Lyon (‰)
δ44/42Ca SRM915a (‰)
−1.25
−1.50
−1.75
−2.00
−0.7
−0.9
−1.1
−1.3
−1.5
0
10
20
30
Age (month)
DP4
M2
P4
M1
M3

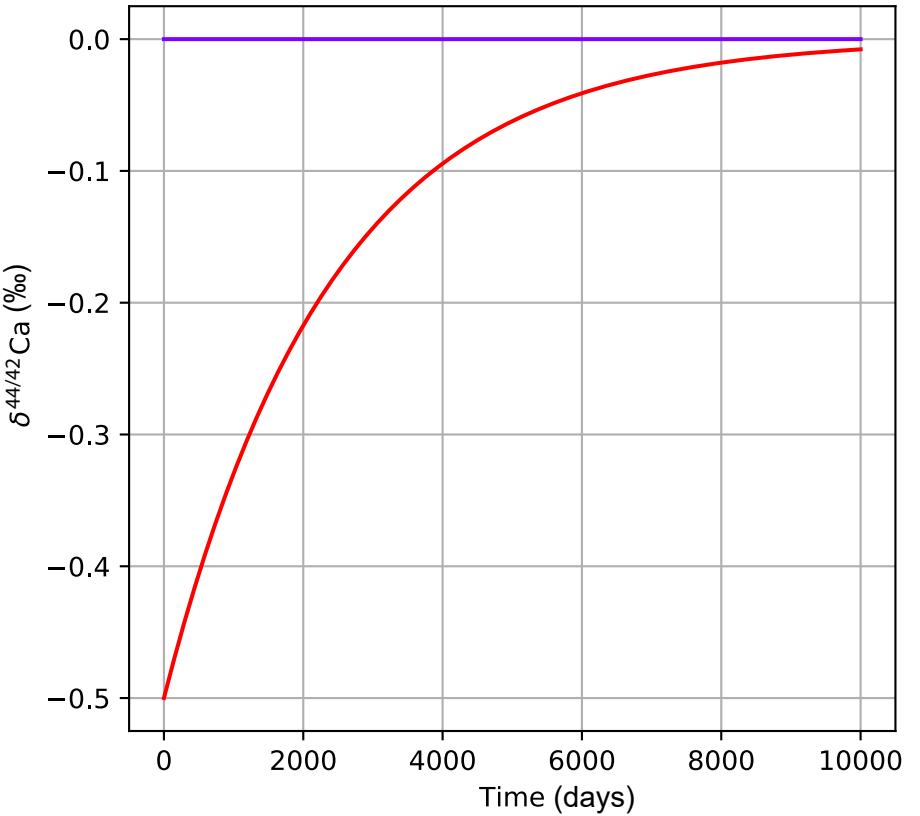
0.0
−0.1
−0.2
−0.3
−0.4
−0.5
$\delta^{44/42}$Ca (‰)
0
2000
4000
6000
8000
10000
Time (days)

sex	age	mean	sd	n	lower	upper
F	A	98.05	12.82	447	81.58	114.52
F	J	52.00	8.75	223	40.73	63.27
F	SA	77.21	9.30	102	65.15	89.27
M	A	150.71	27.90	457	114.87	186.56
M	J	56.40	8.70	218	45.20	67.60
M	SA	96.05	13.66	187	78.44	113.66

Collection id	Lab name	Origin	Genus	Species	Tissue
UP-15CE0104	15CE0104 os	Bauges	*Cervus*	*elaphus*	mandibular bone
UP-15CE0106	15CE0106 os	Bauges	*Cervus*	*elaphus*	mandibular bone
UP-15CE0140	15CE0140 os	Bauges	*Cervus*	*elaphus*	mandibular bone
UP-15CE2616	15CE2616 os	Bauges	*Cervus*	*elaphus*	mandibular bone
UP-15CE2620	15CE2620 os	Bauges	*Cervus*	*elaphus*	mandibular bone
UP-15CE2655	15CE2655 os	Bauges	*Cervus*	*elaphus*	mandibular bone
UP-15CE3523	15CE3523 os	Bauges	*Cervus*	*elaphus*	mandibular bone
UP-15CE4526	15CE4526 os	Bauges	*Cervus*	*elaphus*	mandibular bone
UP-15CE4821	15CE4821 os	Bauges	*Cervus*	*elaphus*	mandibular bone
UP-15CE4823	15CE4823 os	Bauges	*Cervus*	*elaphus*	mandibular bone
UP-15CE4825	15CE4825 os	Bauges	*Cervus*	*elaphus*	mandibular bone
UP-15CE4929	15CE4929 os	Bauges	*Cervus*	*elaphus*	mandibular bone
UP-15CE4951	15CE4951 os	Bauges	*Cervus*	*elaphus*	mandibular bone
UP-15CE5028	15CE5028 os	Bauges	*Cervus*	*elaphus*	mandibular bone
UP-15CE5519	15CE5519 os	Bauges	*Cervus*	*elaphus*	mandibular bone
UP-15CE5616	15CE5616 os	Bauges	*Cervus*	*elaphus*	mandibular bone
UP-15CE5795	15CE5795 os	Bauges	*Cervus*	*elaphus*	mandibular bone
UP-15CE5837	15CE5837 os	Bauges	*Cervus*	*elaphus*	mandibular bone
UP-15CE7104	15CE7104 os	Bauges	*Cervus*	*elaphus*	mandibular bone
UP-15CE5672	AB M1-3	Bauges	*Cervus*	*elaphus*	enamel
UP-15CE5672	AB M1-4	Bauges	*Cervus*	*elaphus*	enamel
UP-15CE5672	AB M1-5	Bauges	*Cervus*	*elaphus*	enamel
UP-15CE5672	AB M1-11	Bauges	*Cervus*	*elaphus*	enamel
UP-15CE5672	AB M1-12	Bauges	*Cervus*	*elaphus*	enamel
UP-15CE5672	AB M1-13	Bauges	*Cervus*	*elaphus*	enamel
UP-15CE5672	AB M1-7	Bauges	*Cervus*	*elaphus*	enamel
UP-15CE5672	AB M2-1	Bauges	*Cervus*	*elaphus*	enamel
UP-15CE5672	AB M2-2	Bauges	*Cervus*	*elaphus*	enamel
UP-15CE5672	AB M2-3	Bauges	*Cervus*	*elaphus*	enamel
UP-15CE5672	AB M2-4	Bauges	*Cervus*	*elaphus*	enamel
UP-15CE5672	AB M2-5	Bauges	*Cervus*	*elaphus*	enamel
UP-15CE5672	AB M2-6	Bauges	*Cervus*	*elaphus*	enamel
UP-15CE5672	AB M3-1	Bauges	*Cervus*	*elaphus*	enamel
UP-15CE5672	AB M3-2	Bauges	*Cervus*	*elaphus*	enamel
UP-15CE5672	AB M3-3	Bauges	*Cervus*	*elaphus*	enamel
UP-15CE5672	AB os	Bauges	*Cervus*	*elaphus*	mandibule bone
UP-15CE3734	JVB DP4-1	Bauges	*Cervus*	*elaphus*	enamel
UP-15CE3734	JVB DP4-2	Bauges	*Cervus*	*elaphus*	enamel
UP-15CE3734	JVB M1-1	Bauges	*Cervus*	*elaphus*	enamel
UP-15CE3734	JVB M1-2	Bauges	*Cervus*	*elaphus*	enamel
UP-15CE3734	JVB M1-3	Bauges	*Cervus*	*elaphus*	enamel
UP-15CE3734	JVB M1-4	Bauges	*Cervus*	*elaphus*	enamel
UP-15CE3734	JVB M1-5	Bauges	*Cervus*	*elaphus*	enamel
UP-15CE3734	JVB M1-6	Bauges	*Cervus*	*elaphus*	enamel
UP-15CE3734	JVB M1-7	Bauges	*Cervus*	*elaphus*	enamel
UP-15CE3734	JVB M2-1	Bauges	*Cervus*	*elaphus*	enamel
UP-15CE3734	JVB M2-2	Bauges	*Cervus*	*elaphus*	enamel
UP-15CE3734	JVB M3-1	Bauges	*Cervus*	*elaphus*	enamel

UP-15CE3734	JVB M3-2	Bauges	*Cervus*	*elaphus*	enamel
UP-15CE3734	JVB os	Bauges	*Cervus*	*elaphus*	mandibule bone
MHNL-50002207	SPB B1	Europe	*Cervus*	*elaphus*	antler bone
MHNL-50002207	SPB B2	Europe	*Cervus*	*elaphus*	antler bone
MHNL-50002207	SPB B3	Europe	*Cervus*	*elaphus*	antler bone
MHNL-50002207	SPB os	Europe	*Cervus*	*elaphus*	mandibule bone

Sampling technique	Age [year]	Sex	ath.date [m/c	Gutted.weight [kg]
handed drill	≥3	female	10/31/2015	61
handed drill	≥3	male	10/18/2015	87
handed drill	≥3	male	12/06/2015	142
handed drill	≥3	male	10/26/2015	na
handed drill	≥3	male	11/22/2015	149.5
handed drill	≥3	male	10/24/2015	na
handed drill	**2**	female	10/25/2015	na
handed drill	≥3	female	11/08/2015	72.1
handed drill	≥3	female	10/22/2015	42
handed drill	≥3	female	11/15/2015	70
handed drill	≥3	female	10/22/2015	48
handed drill	≥3	female	10/22/2015	48
handed drill	≥3	female	11/22/2015	75.5
handed drill	**2**	female	11/01/2015	na
handed drill	**2**	male	10/01/2015	70
handed drill	≥3	male	11/12/2015	132.5
handed drill	**2**	male	10/27/2015	na
handed drill	≥3	male	11/15/2015	122.5
handed drill	≥3	female	10/31/2015	na
edge-drilling procedure	≥3	male	12/20/2015	90.5
edge-drilling procedure	≥3	male	12/20/2015	90.5
edge-drilling procedure	≥3	male	12/20/2015	90.5
edge-drilling procedure	≥3	male	12/20/2015	90.5
edge-drilling procedure	≥3	male	12/20/2015	90.5
edge-drilling procedure	≥3	male	12/20/2015	90.5
edge-drilling procedure	≥3	male	12/20/2015	90.5
edge-drilling procedure	≥3	male	12/20/2015	90.5
edge-drilling procedure	≥3	male	12/20/2015	90.5
edge-drilling procedure	≥3	male	12/20/2015	90.5
edge-drilling procedure	≥3	male	12/20/2015	90.5
edge-drilling procedure	≥3	male	12/20/2015	90.5
edge-drilling procedure	≥3	male	12/20/2015	90.5
edge-drilling procedure	≥3	male	12/20/2015	90.5
edge-drilling procedure	≥3	male	12/20/2015	90.5
edge-drilling procedure	≥3	male	12/20/2015	90.5
handed drill	≥3	male	12/20/2015	90.5
outer-drilling procedure	**2**	female	10/17/2015	70
outer-drilling procedure	**2**	female	10/17/2015	70
edge-drilling procedure	**2**	female	10/17/2015	70
edge-drilling procedure	**2**	female	10/17/2015	70
edge-drilling procedure	**2**	female	10/17/2015	70
edge-drilling procedure	**2**	female	10/17/2015	70
edge-drilling procedure	**2**	female	10/17/2015	70
edge-drilling procedure	**2**	female	10/17/2015	70
edge-drilling procedure	**2**	female	10/17/2015	70
outer-drilling procedure	**2**	female	10/17/2015	70
outer-drilling procedure	**2**	female	10/17/2015	70
outer-drilling procedure	**2**	female	10/17/2015	70

outer-drilling procedure	**2**	female	10/17/2015	70
handed drill	**2**	female	10/17/2015	70
handed drill	≥3	male	na	na
handed drill	≥3	male	na	na
handed drill	≥3	male	na	na
handed drill	≥3	male	na	na

total.body.mass [kg]	n	Mean $\delta^{44/42}Ca$	Mean $\delta^{43/42}Ca$	Mean $\delta^{44/43}Ca$	rel to ICP Ca Lyon 2 s.d. $\delta^{44/42}Ca$
86.62	2	-1.22	-0.61	-0.61	0.04
111.36	2	-1.32	-0.66	-0.67	0.03
190	4	-1.43	-0.70	-0.72	0.07
142	2	-1.40	-0.68	-0.72	0.11
191.5	2	-1.53	-0.75	-0.78	0.10
145	2	-1.61	-0.78	-0.83	0.01
61	2	-1.44	-0.70	-0.73	0.08
102.382	2	-1.30	-0.64	-0.66	0.15
59.64	2	-1.52	-0.75	-0.77	0.01
99.4	3	-1.33	-0.64	-0.70	0.07
68.16	2	-1.24	-0.61	-0.64	0.01
68.16	2	-1.27	-0.60	-0.68	0.01
107.21	2	-1.49	-0.72	-0.78	0.04
72.5	2	-1.55	-0.76	-0.79	0.18
89.6	2	-1.36	-0.64	-0.70	0.06
169.6	2	-1.27	-0.63	-0.64	0.04
76	2	-1.24	-0.60	-0.63	0.01
155	3	-1.62	-0.82	-0.80	0.19
85	2	-1.24	-0.60	-0.63	0.39
115.84	2	-1.44	-0.74	-0.69	0.01
115.84	3	-1.47	-0.74	-0.72	0.03
115.84	2	-1.44	-0.73	-0.72	0.01
115.84	4	-1.54	-0.82	-0.73	0.04
115.84	3	-1.50	-0.76	-0.75	0.04
115.84	4	-1.54	-0.80	-0.75	0.04
115.84	2	-1.66	-0.88	-0.78	0.08
115.84	2	-1.27	-0.62	-0.65	0.02
115.84	2	-1.26	-0.62	-0.64	0.08
115.84	2	-1.35	-0.69	-0.66	0.15
115.84	2	-1.35	-0.69	-0.67	0.16
115.84	2	-1.36	-0.67	-0.69	0.05
115.84	2	-1.34	-0.66	-0.69	0.09
115.84	2	-1.37	-0.70	-0.67	0.03
115.84	2	-1.36	-0.67	-0.68	0.17
115.84	2	-1.33	-0.67	-0.67	0.00
115.84	5	-1.36	-0.66	-0.70	0.17
99.4	3	-1.60	-0.80	-0.81	0.08
99.4	3	-1.62	-0.79	-0.83	0.04
99.4	3	-1.60	-0.80	-0.79	0.05
99.4	3	-1.57	-0.79	-0.78	0.04
99.4	3	-1.57	-0.79	-0.78	0.04
99.4	3	-1.61	-0.81	-0.81	0.07
99.4	3	-1.61	-0.81	-0.80	0.10
99.4	4	-1.66	-0.82	-0.83	0.07
99.4	4	-1.74	-0.87	-0.87	0.03
99.4	3	-1.43	-0.70	-0.72	0.05
99.4	5	-1.53	-0.76	-0.77	0.12
99.4	3	-1.38	-0.69	-0.69	0.11

	99.4	4	-1.59	-0.80	-0.79	0.09
	99.4	4	-1.37	-0.67	-0.68	0.08
na		4	-1.43	-0.71	-0.72	0.02
na		4	-1.38	-0.69	-0.68	0.06
na		3	-1.49	-0.73	-0.75	0.06
na		3	-1.62	-0.79	-0.82	0.04

2 s.d. $\delta^{43/42}Ca$	2 s.d. $\delta^{44/43}Ca$	rel to SRM915a Mean $\delta^{44/42}Ca$
0.08	0.01	-0.70
0.01	0.02	-0.80
0.05	0.05	-0.91
0.04	0.10	-0.88
0.03	0.14	-1.02
0.08	0.06	-1.09
0.10	0.00	-0.92
0.09	0.06	-0.79
0.01	0.01	-1.00
0.01	0.07	-0.82
0.05	0.02	-0.73
0.00	0.01	-0.75
0.06	0.02	-0.97
0.07	0.12	-1.03
0.03	0.00	-0.84
0.04	0.09	-0.75
0.01	0.01	-0.72
0.12	0.11	-1.10
0.22	0.16	-0.72
0.04	0.03	-0.92
0.08	0.03	-0.95
0.04	0.04	-0.92
0.07	0.05	-1.03
0.04	0.02	-0.98
0.06	0.07	-1.02
0.01	0.07	-1.14
0.06	0.01	-0.75
0.06	0.02	-0.74
0.08	0.06	-0.83
0.00	0.09	-0.83
0.01	0.03	-0.84
0.10	0.00	-0.82
0.10	0.07	-0.85
0.14	0.01	-0.84
0.03	0.00	-0.81
0.09	0.09	-0.84
0.04	0.03	-1.08
0.06	0.07	-1.10
0.06	0.08	-1.08
0.02	0.04	-1.05
0.05	0.01	-1.05
0.04	0.06	-1.09
0.04	0.05	-1.09
0.08	0.01	-1.14
0.03	0.02	-1.22
0.03	0.04	-0.91
0.09	0.05	-1.01
0.07	0.05	-0.86

0.07	0.02	-1.07
0.05	0.07	-0.85
0.02	0.04	-0.92
0.07	0.02	-0.87
0.04	0.06	-0.98
0.02	0.04	-1.10

Collection id	Lab name	Origin	Genus	Species	Tissue
UCBL-FSL 451.409	AJ M1-1	Jaurens	*Rangifer*	*tarandus*	enamel
FSL 451.409	AJ M1-2	Jaurens	*Rangifer*	*tarandus*	enamel
FSL 451.409	AJ M1-3	Jaurens	*Rangifer*	*tarandus*	enamel
FSL 451.409	AJ M2-1	Jaurens	*Rangifer*	*tarandus*	enamel
FSL 451.409	AJ M2-2	Jaurens	*Rangifer*	*tarandus*	enamel
FSL 451.409	AJ M2-3	Jaurens	*Rangifer*	*tarandus*	enamel
FSL 451.409	AJ M3-1	Jaurens	*Rangifer*	*tarandus*	enamel
FSL 451.409	AJ M3-2	Jaurens	*Rangifer*	*tarandus*	enamel
FSL 451.409	AJ M3-3	Jaurens	*Rangifer*	*tarandus*	enamel
FSL 451.409	AJ os	Jaurens	*Rangifer*	*tarandus*	mandibule bone
FSL 451.409	AJ P3-1	Jaurens	*Rangifer*	*tarandus*	enamel
FSL 451.409	AJ P3-2	Jaurens	*Rangifer*	*tarandus*	enamel
FSL 451.409	AJ P3-3	Jaurens	*Rangifer*	*tarandus*	enamel
FSL 451.398	ISO DP4-1	Jaurens	*Rangifer*	*tarandus*	enamel
FSL 451.398	ISO DP4-5	Jaurens	*Rangifer*	*tarandus*	enamel
FSL 451.384	ISO M1-1	Jaurens	*Rangifer*	*tarandus*	enamel
FSL 451.384	ISO M1-2	Jaurens	*Rangifer*	*tarandus*	enamel
FSL 451.384	ISO M1-3	Jaurens	*Rangifer*	*tarandus*	enamel
FSL 451.384	ISO M1-4	Jaurens	*Rangifer*	*tarandus*	enamel
FSL 451.384	ISO M1-5	Jaurens	*Rangifer*	*tarandus*	enamel
FSL 451.384	ISO M1-6	Jaurens	*Rangifer*	*tarandus*	enamel
FSL 451.384	ISO M1-7	Jaurens	*Rangifer*	*tarandus*	enamel
FSL 451.389	JVJ DP4-1	Jaurens	*Rangifer*	*tarandus*	enamel
FSL 451.389	JVJ DP4-2	Jaurens	*Rangifer*	*tarandus*	enamel
FSL 451.389	JVJ DP4-3	Jaurens	*Rangifer*	*tarandus*	enamel
FSL 451.389	JVJ M1-1	Jaurens	*Rangifer*	*tarandus*	enamel
FSL 451.389	JVJ M1-2	Jaurens	*Rangifer*	*tarandus*	enamel
FSL 451.389	JVJ M1-3	Jaurens	*Rangifer*	*tarandus*	enamel
FSL 451.389	JVJ M1-4	Jaurens	*Rangifer*	*tarandus*	enamel
FSL 451.389	JVJ M1-5	Jaurens	*Rangifer*	*tarandus*	enamel
FSL 451.389	JVJ M1-6	Jaurens	*Rangifer*	*tarandus*	enamel
FSL 451.389	JVJ M2-1	Jaurens	*Rangifer*	*tarandus*	enamel
FSL 451.389	JVJ os	Jaurens	*Rangifer*	*tarandus*	mandibular bone

Sampling technique	n	rel to ICP Ca Lyon			
		Mean $\delta^{44/42}Ca$	Mean $\delta^{43/42}Ca$	Mean $\delta^{44/43}Ca$	2 s.d. $\delta^{44/42}Ca$
outer-drilling procedure	3	-1.52	-0.82	-0.71	0.09
outer-drilling procedure	3	-1.43	-0.75	-0.67	0.06
outer-drilling procedure	3	-1.55	-0.83	-0.71	0.05
outer-drilling procedure	3	-1.67	-0.88	-0.78	0.02
outer-drilling procedure	3	-1.62	-0.84	-0.78	0.06
outer-drilling procedure	3	-1.48	-0.74	-0.73	0.01
outer-drilling procedure	3	-1.64	-0.89	-0.76	0.04
outer-drilling procedure	3	-1.48	-0.74	-0.75	0.03
outer-drilling procedure	3	-1.47	-0.77	-0.71	0.04
outer-drilling procedure	5	-1.00	-0.49	-0.50	0.14
outer-drilling procedure	3	-1.68	-0.87	-0.80	0.01
outer-drilling procedure	3	-1.61	-0.84	-0.76	0.04
outer-drilling procedure	3	-1.49	-0.75	-0.75	0.09
edge-drilling procedure	2	-1.90	-0.97	-0.93	0.07
edge-drilling procedure	3	-1.74	-0.90	-0.84	0.05
edge-drilling procedure	4	-1.48	-0.75	-0.73	0.08
edge-drilling procedure	4	-1.39	-0.71	-0.68	0.09
edge-drilling procedure	2	-1.55	-0.76	-0.76	0.05
edge-drilling procedure	2	-1.57	-0.81	-0.77	0.07
edge-drilling procedure	3	-1.68	-0.84	-0.84	0.09
edge-drilling procedure	3	-1.65	-0.83	-0.81	0.04
edge-drilling procedure	3	-1.85	-0.96	-0.90	0.09
outer-drilling procedure	3	-1.95	-1.03	-0.92	0.07
outer-drilling procedure	3	-1.91	-0.97	-0.92	0.03
outer-drilling procedure	3	-1.97	-0.98	-0.99	0.10
outer-drilling procedure	3	-1.21	-0.62	-0.60	0.03
outer-drilling procedure	3	-1.68	-0.89	-0.80	0.07
outer-drilling procedure	3	-1.96	-1.05	-0.92	0.06
outer-drilling procedure	2	-1.68	-0.86	-0.82	0.03
outer-drilling procedure	2	-1.75	-0.89	-0.85	0.07
outer-drilling procedure	2	-2.03	-1.03	-0.99	0.08
outer-drilling procedure	4	-1.52	-0.76	-0.75	0.15
outer-drilling procedure	3	-0.94	-0.47	-0.48	0.17

2 s.d. $\delta^{43/42}Ca$	2 s.d. $\delta^{44/43}Ca$	rel to SRM915a Mean $\delta^{44/42}Ca$
0.01	0.08	-1.00
0.14	0.08	-0.92
0.13	0.15	-1.03
0.08	0.11	-1.15
0.10	0.02	-1.10
0.01	0.05	-0.96
0.08	0.06	-1.13
0.03	0.05	-0.97
0.04	0.04	-0.95
0.10	0.06	-0.48
0.04	0.08	-1.16
0.04	0.04	-1.09
0.15	0.07	-0.98
0.10	0.03	-1.38
0.04	0.04	-1.22
0.06	0.07	-0.96
0.12	0.04	-0.87
0.05	0.02	-1.03
0.02	0.09	-1.05
0.03	0.04	-1.17
0.07	0.04	-1.13
0.07	0.06	-1.34
0.05	0.04	-1.43
0.01	0.04	-1.39
0.12	0.02	-1.45
0.06	0.07	-0.69
0.12	0.07	-1.16
0.06	0.10	-1.44
0.03	0.02	-1.16
0.02	0.07	-1.23
0.10	0.01	-1.51
0.12	0.06	-1.00
0.09	0.08	-0.42

Standard name	Provider	Study
SRM1486	NIST	this study
		Martin et al. 2018
		Tacail et al. 2017
		Tacail et al. 2016
		Heuser and Eisenhauer 2008
IAPSO	OSIL	this study
		Martin et al. 2015
		Tacail et al. 2014
		Compiled in Martin et al. 2015 from 16 studies

Standard conversions

All standards and datasets from the literature expressed in $\delta^{44/40}$Ca values were converted to $\delta^{44/42}$C
The constant difference of – 0.518 ± 0.025 ‰ between standards measured against SRM915a versu

n	$\delta^{44/42}Ca_{ICP\ Ca\ Lyon}$	2 s.d.
88	-1.00	0.07
101	-1.05	0.13
147	-1.03	0.12
120	-1.03	0.13
142	-1.02	0.12
14	0.38	0.06
5	0.41	0.12
2	0.41	0.06
-	0.41	0.07

Ca by dividing by 2.048, as calculated using the exponential mass dependent fractionation law (supple
us ICP Ca Lyon (supplementaries from Martin et al. 2018) was used to calculate the corresponding iso

ementaries from Martin et al. 2018).
otope compositions of international standards from the literature with respect to ICP Ca Lyon.

Collection id	Lab name	Origin	Genus	Species	sample type	ca [%]
MNHL-50002207	SPB B1	Europe	*Cervus*	*elaphus*	antler bone	14.56
MNHL-50002207	SPB B2	Europe	*Cervus*	*elaphus*	antler bone	8.99
MNHL-50002207	SPB B3	Europe	*Cervus*	*elaphus*	antler bone	12.43
MNHL-50002207	SPB os	Europe	*Cervus*	*elaphus*	mandibular bone	22.99
FSL 451.409 os	AJ os	Jaurens	*Rangifer*	*tarandus*	mandibular bone	27.87
FSL 451.389 os	JVJ os	Jaurens	*Rangifer*	*tarandus*	mandibular bone	27.32
UP-15CE3734	JVB os	Bauges	*Cervus*	*elaphus*	mandibular bone	21.29
AB F	AB F	Bauges			grass	1.83
JVB F	JVB F	Bauges			grass	0.99

* : below detection limit

p [%]	fe [ppm]	s [ppm]	al [ppm]	ba [ppm]	k [ppm]
7.83	*	6100.1	*	50.1	*
5.10	*	11481.3	*	61.0	2933.5
6.61	*	8465.3	*	39.6	1098.6
11.86	*	8969.5	*	87.7	176.8
13.49	5408.1	2250.0	1838.7	161.7	*
13.71	*	2306.2	1518.7	172.8	*
11.56	*	2181.3	*	98.7	387.0
0.54	313.1	1554.3	223.5	35.4	1298.1
0.50	279.6	2126.6	*	8.8	1419.5

mg [ppm]	mn [ppm]	na [ppm]	sr [ppm]	y [ppm]	la [ppm]
1953.0	13.5	3994.7	116.7	*	9.1
1800.2	11.8	11011.2	58.4	*	8.7
2978.1	2.5	7272.7	57.7	*	5.4
3876.6	13.2	7861.5	126.0	*	4.9
658.5	1696.6	3256.0	109.5	46.8	35.7
638.9	15.1	3150.4	119.5	14.3	18.6
6580.1	1.0	6996.0	110.8	*	5.7
1095.1	219.6	2965.4	23.2	*	1.4
826.5	30.7	4642.3	21.6	*	1.4

ce [ppm]	pr [ppm]	nd [ppm]	sm [ppm]	eu [ppm]	gd [ppm]	tb [ppm]
*	*	*	*	*	*	*
*	*	*	*	*	*	*
*	*	*	*	*	*	*
*	*	*	*	*	*	*
12.1	4.8	23.3	3.6	0.9	4.1	*
1.6	1.5	7.6	1.0	*	1.3	*
*	*	*	*	*	*	*
*	*	*	*	*	*	*
*	*	*	*	*	*	*

dy [ppm]	ho [ppm]	er [ppm]	tm [ppm]	yb [ppm]	lu [ppm]
*	*	*	*	*	*
*	*	*	*	*	*
*	*	*	*	*	*
*	*	*	*	*	*
3.0	0.8	2.3	*	2.0	*
*	*	*	*	*	*
*	*	*	*	*	*
*	*	*	*	*	*
*	*	*	*	*	*